Quantifying the effects of near surface density variation on quantum technology gravity and gravity gradient instruments

Boddice, Daniel; Metje, Nicole; Tuckwell, George

DOI:
10.1016/j.jappgeo.2019.03.012

Quantifying the Effects of Near Surface Density Variation on Quantum Technology Gravity and Gravity Gradient Instruments

Daniel Boddice[1*], Nicole Metje[1], George Tuckwell[1, 2]

1. School of Engineering, College of Engineering and Physical Sciences, University of Birmingham, Edgbaston, Birmingham, B15 2TT
2. RSK, 18 Frogmore Road, Hemel Hempstead, Hertfordshire, HP3 9RT, UK

* Corresponding author; email:d.boddice@bham.ac.uk

Abstract

Natural density variations in the near surface soil (i.e. the top 5 m) cause variations in the values recorded by geophysical surveys undertaken with gravity instruments. Whilst this 'soil noise' is too small to be noticeable with current instruments (e.g. Scintrex CG-5 and CG-6), the future use of more accurate instruments such as quantum technology gravity sensors, especially if used in a gradiometer configuration makes this noise source more significant and in need of characterisation and quantification. This paper reviews the magnitude and distribution of density variations in the near surface using data from the British Geological Survey (BGS) national geotechnical properties database which is then used to quantify the effect on practical gravity measurements in computer simulations.

The desk study identified that the scale of density variation in the near surface was typically within a range of 600-900 kg/m^3, and showed no obvious relationship with underlying geology, superficial deposits or depth below the surface. The distribution of density varied, from normally distributed to between normal and uniform or bimodal distributions. The forward modelled computer simulations showed a significant impact on the measurements of gravity if new instruments can reach greater levels of accuracy, especially for gravity gradient instruments. Analysing possible methods of suppressing this noise source through the design of gravity gradient instruments showed that, although increasing the height of the instrument above the ground is almost twice as effective at decreasing the scale of the soil noise, increasing the sensor vertical spacing may be the preferred option. This is due to relaxed sensitivity requirements on the new sensors and the preservation of the noise in shorter signal wavelength bands than the targets of interest, which not only reduces the

cases of mistaken features of interest but also provides the possibility of spatial filtering to be used in order to enhance the signals from targets of interest.

Keywords: Gravity, Gravity gradient, Noise quantification, Quantum technology

1. Introduction

Geophysical techniques which respond to the physical properties of the soil are widely used to look through the soil in order to find buried targets. However, the near surface soil (i.e. the top 5 m) is inherently heterogeneous and contains spatial variations in its measured geophysical properties giving rise to small anomalies on the final geophysical data map which can mask the signal from the target of interest. This 'soil noise' presents an interesting challenge for future gravity surveys as variations in near surface density generate gravitational signals. Whilst work has been carried out to quantify the scale of the soil noise for magnetic and electromagnetic measurements (Hendrickx et al., 2001; Van Dam et al., 2004), no work has been conducted to quantify variations in near surface density which affect measurements with gravity instruments. Current spring based gravimeters (such as the Scintrex CG-5 and CG-6) have a nominal resolution of 1 μGal and 0.1 μGal respectively, but in practical applications are typically only capable of a practical resolution of ±5 μGal with realistic integration times in field conditions (Boddice et al., 2018; Jiang et al., 2012; Tuckwell et al., 2008) due to the presence of environmental and instrumental noise. This means the contribution of soil density variations to the recorded gravity map is too small to be concerned with in current microgravity surveys, and separating these effects from the instrument and other environmental sources of noise which limit the practical resolution for feature detection is difficult. However, more accurate instruments in development, based on quantum technology (QT) (Hinton et al., 2017) promise a revolution in sensor resolution and precision, allowing the soil noise to be detected above the inherent instrument noise, and thus making these effects significant when using microgravity surveys to locate buried targets. Furthermore, previous research also demonstrated that these instruments should be operated in a gradiometer configuration in order to make the most of this extra

sensitivity and cancel environmental sources of noise (Boddice, Metje and Tuckwell, 2017). However, due to the proximity of the bottom sensor to the ground and the strong drop off in signal strength with distance, large differences in signal strength between the top and bottom sensor make the effects of near surface soil noise more significant. It has also been identified that soil noise is significant in the inversion of gravity and gravity gradient data (Brown et al., 2016) as it increases the uncertainty of the individual measurement points and thus the range of plausible solutions. The effects were modelled on synthetic data using a spatially correlated soil noise model to take these effects into account. However, the authors noted that they were unsure as to how well this model of density noise was representative of reality and the true scale of these density variations in real world conditions.

To identify the potential of this noise to mask signals from deeper features of interest when using these instruments, some assessment needs to be made on the scale and distribution of density variation and quantification of its effect on the resulting gravity and gravity gradient signals. Although density testing is often carried out as part of soil characterisation tests in civil engineering, no published examples have been found discussing the variability of soil density on the scale of a typical survey site (between a few tens and a few hundred square metres). Several reasons exist for this:

1. Existing methods for testing soil density for both laboratory and field applications yield a significant variation in density values and as a result require averaging several samples. For example, laboratory civil engineering applications use water displacement on undisturbed samples of soil to determine the volume (BSI, 1990), with multiple readings averaged to account for the limited precision of the method.

As these methods are destructive to the samples, the values derived are made from multiple samples, which averages out lots of the spatial density variability which would affect gravity measurements. To the authors knowledge, no quantification of the repeatability of these methods has been published, although repeatability analysis for soil compaction (Sherwood, 1970) has been suggested as a reasonable proxy and shows substantial errors of 10 – 20 kg/m^3 in the final results even after multiple averages.

2. Density values recorded and quoted for civil engineering applications typically represent the dry density of the soil in order to make the results of different soils directly comparable, regardless of the degree of saturation. However, wet bulk density variations in-situ which would affect gravity results are often not recorded and may vary depending on the weather and prevailing environmental conditions.
3. Boreholes and density test samples collected during engineering work are usually spaced too far apart to be of use for assessing variation in the near surface over the scale of a typical engineering survey site at the spacing required for direct application to a dense grid of gravity measurements.

This paper aims to quantify soil density variation in the near surface and the resulting effects on high accuracy gravity and gravity gradient surveys (for example using QT instruments). To achieve this, two methods will be used. Firstly, borehole records collected from the BGS databases for the top few metres containing density information are used to assess the scale and distribution of density variation on a site specific scale. Secondly, simulations are performed to establish the potential effect of these variations on gravity.

2. Quantum Technology Gravity Gradiometers

The standard measurement approach for a microgravity survey is to employ a mass-on-spring system, where gravity is measured through observing the force on the spring such as with the Scintrex CG-5 and CG-6. An alternative approach is to drop or throw a test-mass and observe its travel through the gravitational field such as in falling corner cube devices, e.g. the FG5 (Niebauer et al., 1995), but these are currently unsuited to field conditions due to lengthy set-up times and mechanical wear. Atomic quantum technology gravity sensors use the latter approach and measure gravity through putting a small cloud of atoms into free-fall, and observing how they fall in a way that has the potential to be robust enough to be used in a field environment. Gradient measurements can also be taken by using a single laser as a ruler to interrogate two clouds of atoms at different heights simultaneously. To take a measurement, lasers are also used to cool and trap a sample of atoms to a temperature of a billionth of a degree above absolute zero, allowing them to fall with minimal expansion over the measurement time. The trajectory of the cloud of atoms under the influence of gravity is measured using a series of laser pulses, exploiting the principles of quantum superposition to generate interferometric fringes. Demonstrations in laboratories promise 100-1000 fold higher sensitivity than current technology, whereas the use of perfectly identical atoms as test masses and a single laser ruler ensures that measurements are accurate, easily repeatable, drift free, and well correlated in time making them ideal for gradient measurements by using two atom clouds at different heights to facilitate the cancelation of common mode accelerations. The eventual performance is targeted at up to 1 Eötvos resolution. Further details of the operating principles of QT gravity gradiometers can be found in Hinton et al. (2017)

3. Desk Study of Density Variations

In order to obtain quantitative data on the scale and distribution of density variation in the near surface, a desk study was conducted using data acquired from the BGS National Geotechnical properties database (NGPD)[1]. Data with a suitably high concentration of boreholes for the purposes of this study are reasonably rare within the dataset but two areas in the UK with a reasonably high spatial resolution were identified in the review for this work. One area in Glasgow and one covering the East End of London which included a range of geological types and made ground (material artificially placed by anthropogenic activity) were chosen and were assumed to be typically representative of the kind of variation which would be found in any similar size area within the country. The locations of the two study sites are shown in Figure 1. For the borehole records obtained, those which did not contain any information on the density of the soil were removed. The remaining data were used to analyse the density variations.

3.1. Whole Study Areas

Figure 2 shows the density variation and distribution for the two study areas along with a histogram to offer an indication of the distribution and scale of density variations in the near surface. Very similar distributions of density, shown in Figure 2c and f, are recorded in both study areas with only slight variations in average density (approximately 200 kg/m^3 higher in Glasgow than in London). However, the overall density range is similar for both sites (approximately 1200 kg/m^3). In terms of distribution, values for both study areas could be approximated by normal distributions (Figure 2c and f) which had similar standard deviations (wet density SDs were 257 kg/m^3 and 314 kg/m^3 for Glasgow and London respectively). This was confirmed using Levene's Test for equality of variances which

[1] http://www.bgs.ac.uk/services/NGDC/management/geology/geotechnical.html

accepted the null hypothesis (i.e. that the variances were similar) within a confidence of 95% (p-value = 0.138). An independent two sample student t-test between the two datasets rejected the null hypothesis (i.e. that the means of the two groups are equal) with a p-value of 1.57×10^{-273} suggesting the differences between the two study areas are significant, highlighting the need for high accuracy local density information when conducting a microgravity survey, especially for terrain corrections. There are differences in the average value for the wet bulk and dry densities which are statistically significant (Glasgow wet = 1998 kg/m^3 vs dry = 1600 kg/m^3, London wet = 1726 kg/m^3 vs dry = 1223 kg/m^3), with paired student t tests giving p values of < 0.00 for both Glasgow and London. However, absolute density values are unimportant for soil noise, as only variation in density (i.e. the range and distribution of density values) on a given site generate detectable noise signals. Crucially, the spread of values are similar between wet and dry density for both study areas and both can be approximated using a normal distribution which is shown by the lines on Figure 2. The sigma values (wet/dry) are 257/278 kg/m^3 for Glasgow and 314/383 kg/m^3 for London. Whilst this means that the variation is slightly larger for the dry density, which would result in an overestimation of the soil noise, this is preferable to preferable to an underestimation when trying to determine if a target will be visible. It also should be noted that these differences are smaller than the differences between the two study areas suggesting that any available density information is useful for determining the likely effect. This is important as it means that dry density data, which is more commonly recorded in geotechnical databases, can be used as a proxy for the in-situ wet bulk density which affects gravity readings.

In addition to the values of density, equally important for modelling the density variation which causes soil noise is the spatial pattern of density variations, both horizontally and

with depth, and the spatial scale on which the density varies in the ground. The spatial distribution of the density for Glasgow and London are shown in Figure 2a and 2d, respectively. Where samples were taken from multiple depths within the same borehole, an average value has been used. The spatial variation of density across Glasgow shows no clear correlation with the underlying geology or soil types shown in Figure 1. In contrast however, London shows lower density around the river basin which runs through the centre of the site (river shown as area between the black lines), perhaps due to deposits of alluvium which lower the density compared to the surrounding clay. Another possibility is that this is caused by different drainage regimes in the river basin, although spatial analysis of the dry density (not shown in Figures 2a and d) shows similar trends making this unlikely. Examination of the density data by depth (Figure 2b and 2e) shows no relationship between the soil density and the depth below the ground surface in either of the two study areas. In the case of London, this may be due to the effects of the different geological types generating a larger density difference which masks any underlying trends. However, as the same trend is visible in the Glasgow data where no such geologically related trends exist, it is more likely that the variation in density is consistent between depths.

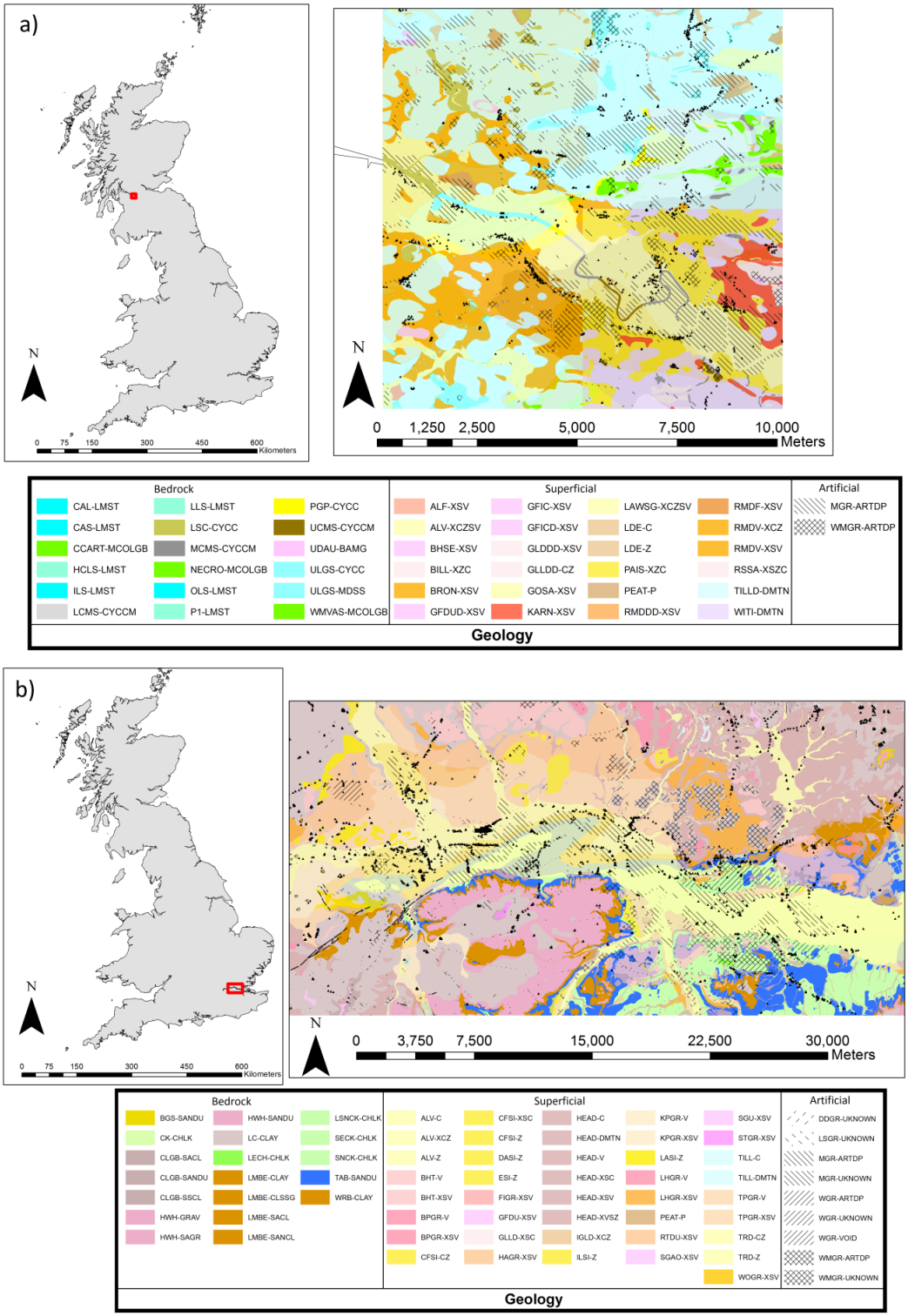

Figure 1: The Location and Geology (described using BGS's Rock Classification scheme[2]) of the Study Data for a) Glasgow and b) London. The Background Geology is a British Geological Survey/EDINA supplied service (British Geological Survey, 2013) and is Crown Copyright/database right 2017. A full list of acronyms is found in the appendix.

[2]Full details can be found at http://www.bgs.ac.uk/bgsrcs/

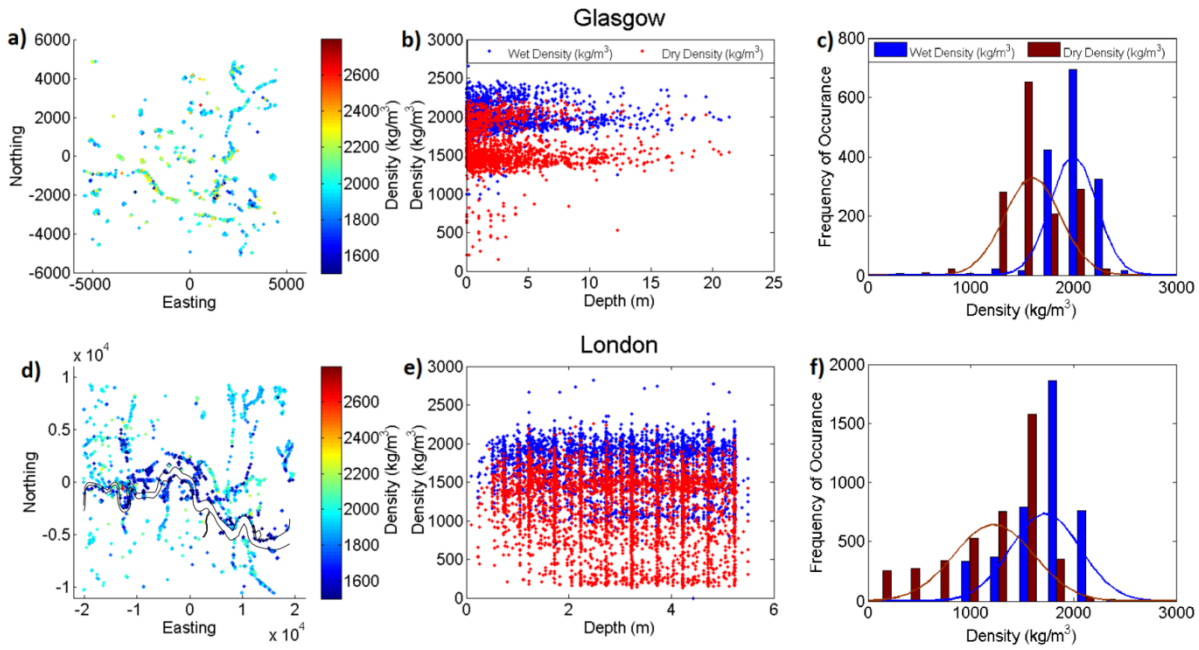

Figure 2: Density data for the two study areas. a) and d) show the spatial trends for density Glasgow and London respectively. b) and e) show the relationship with depth for Glasgow and London respectively and c) and f) show histograms of all the values for Glasgow and London respectively along with normal distributions (denoted by the lines).

3.2. Site Scale Clusters

The study areas are much larger than those covered for a typical geophysical survey for an engineering project (0.01 – 1 km^2), and smaller areas needed to be selected based on clusters of closely spaced boreholes. For each study area, eight clusters of boreholes within an area of a 1 km^2 were selected. Although this would be slightly larger than a typical microgravity survey, especially given the relatively slow speed of the technique, this represents the smallest area within which a reasonable number of samples were available. The locations of these sites for London and Glasgow are shown in Figure 3 and a summary of the locations, geological types and density statistics are provided in Table 1. As can be seen, the sites cover a wide range of different geological and superficial geological types as well as encompassing areas of made ground.

Histograms of the density distributions are shown in Figure 4, along with an ideal normal distribution fit. Approximately half of the study sites can be approximated with a normal distribution (London 1, 5, 6 and 8 and Glasgow 1, 3, 4, 5 and 8). The others have distributions of densities which are less clear but appear as either between uniform and normal distribution (Glasgow 2 and 6 and London 7) or a bimodal distribution (Glasgow 7 and London 2, 3 and 4). However, given the relatively small sample sizes of each of the clusters and the likely physical properties of the soil, it is probable that these dataset are small subsamples of normally distributed datasets. Correlating these distributions to the geology maps shown in Figure 3 shows that the distribution of densities has little correlation with soil types, as even study areas with artificial ground or multiple geologies may display any of the above mentioned distribution patterns, as do single geology type study areas. The results also appear to have no obvious correlation of the distributions with the degree

of fluid saturation, as few differences are apparent in the shape of the distribution between the wet bulk and dry densities. This is important as it shows that the density range does not vary as a response to climatic conditions and therefore the soil noise is likely to remain broadly similar in scale regardless of the time of year. Additionally, it means that the dry density which is more commonly recorded in geotechnical databases can be used as a proxy for the physical property which the gravity instrument detects (i.e. the wet bulk density variation), making prior information about the site before surveying more accessible. The scale of the variation on each of the sites varied from 300 kg/m^3 to 1500 kg/m^3 and averaged around 850 kg/m^3.

As mentioned above, the spatial distribution of density is an important consideration for modelling the effects of gravity soil noise across a site. The spatial distributions of the wet bulk density in the XY plane for the borehole clusters are shown in Figure 5. Examination of this data shows that, for all of the sites, the density varies between even the closest spaced boreholes (the minimum spacing between two boreholes is 2 m in the studied datasets but they are more commonly in the order of tens of metres). This suggests that the wavelength of density variation is almost shorter than a few metres. However, due to the lack of closer spaced boreholes, the precise scale on which density varies could not be determined beyond setting this upper limit. Analysis of these plots alongside the geology maps of the different sites (Figure 3) shows again few trends in the distribution of densities which could be correlated to the types of soil. This was confirmed by multiple linear regression between the X and Y coordinates (independent variables) and the observed density (dependent variable) (Table 2), which showed that the trends were very weak with the only statistically significant trend (95% confidence) being the very weak trend observed on London site 2 (Coefficients of -0.008 and 0.001 with R^2 0.45 and P-value 0.0001). All other sites displayed

insignificant trends (R^2 < 0.29 and P-values > 0.05). No trends are visible in either the distribution or range of values observed on the single geology sites (London 1, 3, 4 and 8 and Glasgow 2, 6 and 7) in comparison to the multiple geological type sites. The relationship between the soil density and depth below the ground surface is shown in Figure 6. As with the study areas as a whole, correlations between the depth of the sample and density are weak for all sites, although some of the sites showed a decrease in the measured density below the top 2 m, for example London, site 4. Linear regression (results shown in Table 3) showed that none of the observed slopes were significantly different to zero using a 5 % confidence margin (p-values of 0.168 - 0.761), with the only exception of London Site 4 (slope coefficient of -0.024, p-value of 0.0008 and adjusted R^2 for the model of 0.23). Visual analysis of this data (Figure 6) shows that the data is divided into two distinct clusters (hence the low R^2 value) which suggests that this relationship is the result of some factor other than the depth, for example a different layer of soil with a lower density below 2 m. These trends are insignificant, and are not consistent between the different study areas.

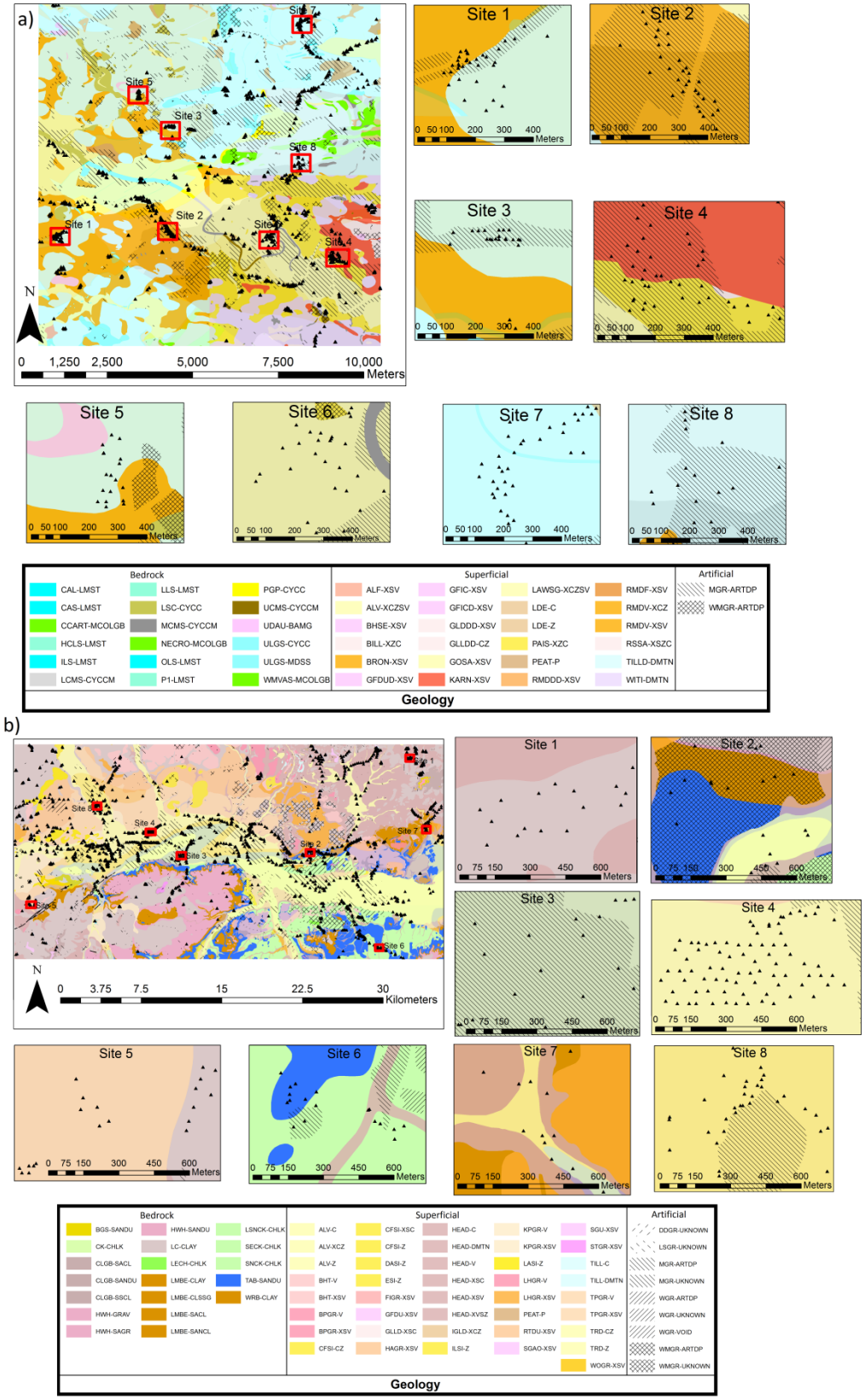

Figure 3: The locations of the study sites in a) Glasgow and b) London. Background Geology is a British Geological Survey/EDINA supplied service (British Geological Survey, 2013). Crown Copyright/database right 2017. A full list of the BGS rock classification scheme abbreviations is given in the appendix.

Table 1: The locations, geology types and density statistics for the different sites chosen. A full list of the BGS rock classification scheme abbreviations is given in an appendix at the end of the paper

Location	Site No	Number of Records	Location		Geology Types (BGS Rock Classification Scheme) (Bedrock *Superficial* ***Artificial***)	Density				
			Easting Extent	Northing Extent		Min Density (kg/m^3)	Max Density (kg/m^3)	Density Range (kg/m^3)	Standard Deviation	Average Density (kg/m^3)
Glasgow	1	67	255362 – 255897	662967 – 663448	LSC-CYCC, *RMDV-XCZ*, *TILLD-DMTN*, **MGR-ARTDP**	1000	2400	1400	270	1910
	2	66	258507 – 259047	663122 – 663597	LCMS-CYCCM, MCMS-CYCCM, *RMDV-XCZ and XSV*, *TILLD-DMTN*, **MGR-ARTDP**	1280	2450	1170	210	2090
	3	61	258584 – 259122	666072 – 666551	LSC-CYCC, *RMDV-XCZ*, *TILLD-DMT*, **MGR-ARTDP**	1780	2440	660	140	1990
	4	55	263421 – 264075	662341 – 662823	MCMS-CYCCM, *KARN-XSV*, *PAIS-XZC*, **MGR-ARTDP**	1340	2460	1120	220	1980
	5	43	257635 – 258173	667112 – 667590	LSC-CYCC, *GFDUD-XSV*, *RMDV-XCZ*, *TILD-DMTN*	1700	2220	520	100	1920
	6	29	261465 – 262003	662868 – 663347	MCMS-CYCCM, *GOSA-XSV*, *PAIS-XZC*, **MGR-ARTDP**, **WMGR-ARTDP**	1240	2410	1170	340	2030
	7	57	262429 – 262970	669174 – 669657	CAL-LMST, ULGS-CYCC, *LDE-C*, *TILLD-DMTN*, **MGR-ARTDP**	1810	2430	620	170	2020
	8	20	262399 – 262941	665124 – 665607	LCMS-CYCCM, MCMS-CYCCM, *RMDV-XCZ*, *TILLD-DMTN*, **MGR-ARTDP**	1760	2380	620	180	2020
London	1	29	566381 – 567139	188435 – 189044	LC-Clay	1510	2080	570	100	1960
	2	33	557108 – 557868	179630 – 180244	HWH-Sandu, LC-CLAY, LMBE-SANCL and SACL, SEC-CHLK, TAB-SANDU, *ALV-Z, HEAD-C, LHGR-XSV,* **MGR-ARTDP, WGR-Unknown, WMGR-ARTDP and UKNOWN**	1070	2170	1100	400	1720
	3	38	545084 – 545922	179345 – 179953	TAB-Sandu, *ALV-Z*, **MGR-ARTDP**	990	2030	1040	330	1440
	4	245	542203 – 543083	181571 – 182135	LC-CLAY, *ALV-Z*	740	2040	1300	290	1320
	5	42	531089 – 531958	174792 – 175357	LC-CLAY, *HEAD-C, TPGR-V and XSV*	1790	2100	310	60	1940
	6	30	563548 – 564283	170787 – 171359	TAB-SANDU, SECK-CHLK, *HEAD-XSC*, **MGR-ARTDP**	1580	2070	490	100	1860
	7	24	567926 – 568669	181762 – 182396	LMBE-SACL, TAB-SANDU, *ALV-Z*, *HEAD-C*, *LHGR-XSV*	1000	1940	940	360	1520
	8	43	537288 – 538030	183968 – 184581	LMBE-Clay, *ALV-C*	1410	2080	670	170	1690

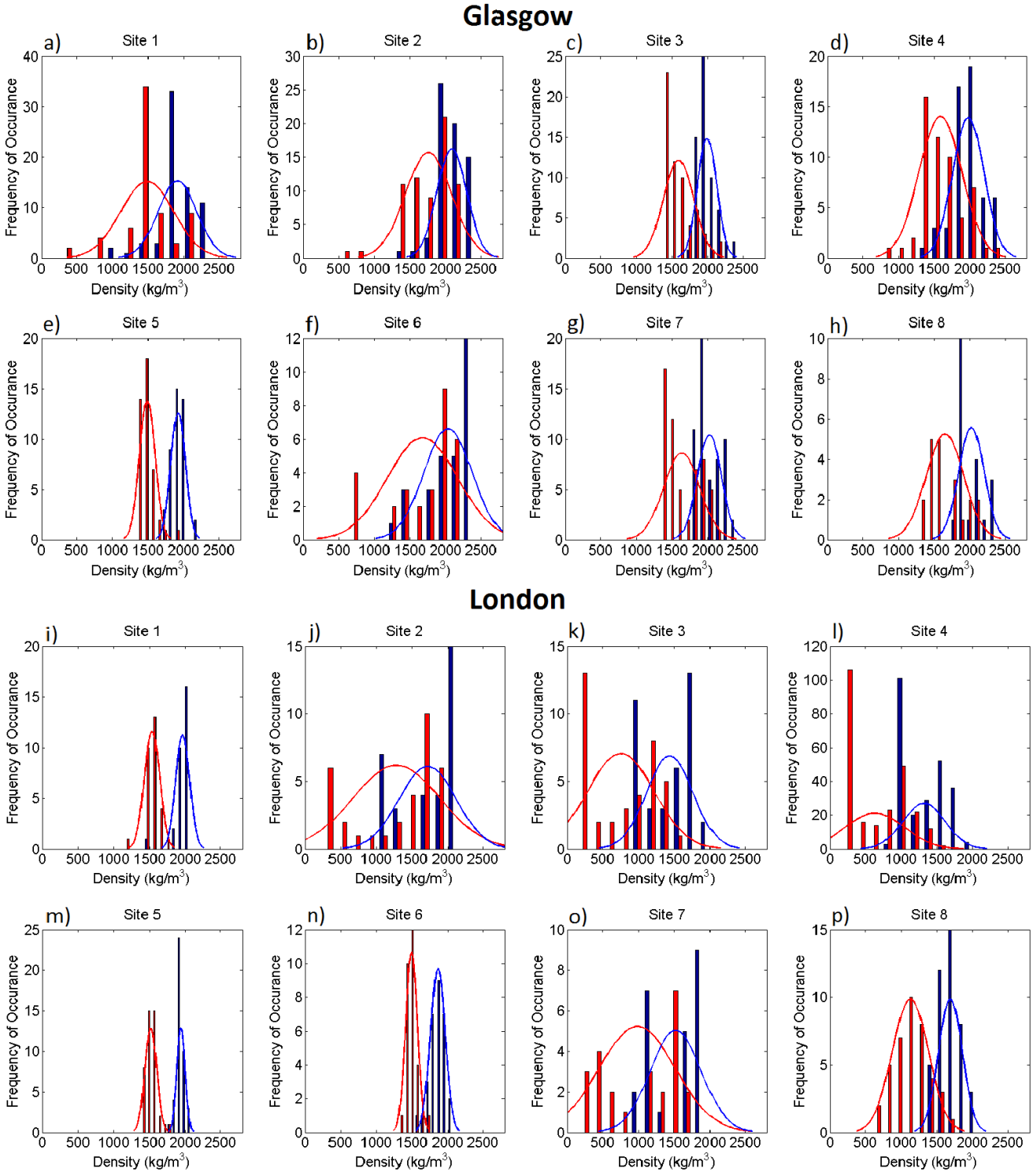

Figure 4: Histograms of the wet (blue) density and dry (red) density recorded for the 8 Glasgow (a-h) and 8 London (i-p) clusters. Normal distributions are denoted by the lines

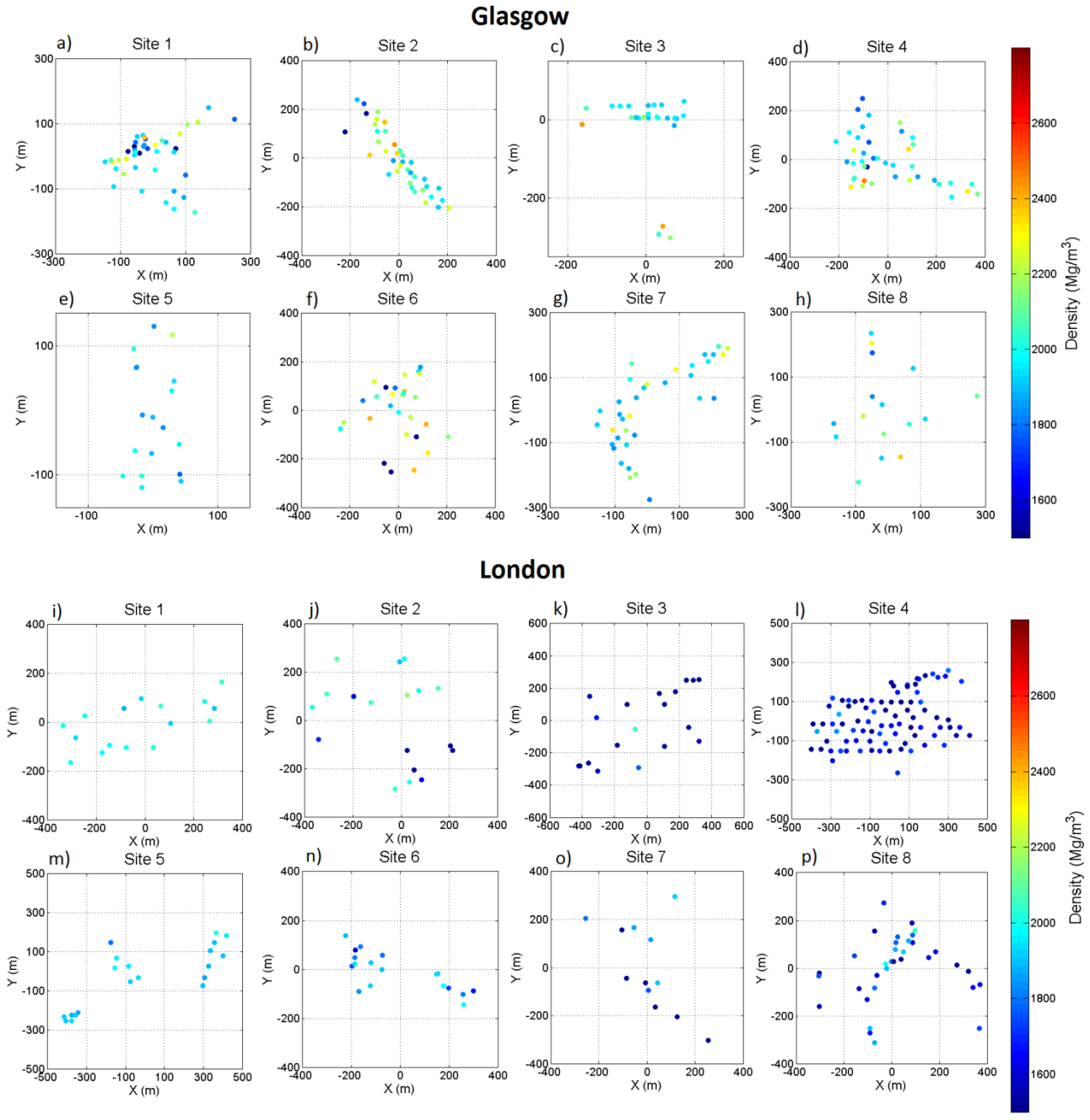

Figure 5: Spatial distribution of density variation for the 8 Glasgow sites (a-h) and 8 London Sites (i-p)

Table 2: Attempted multiple regression between Easting and Northing and density for all of the study sites

	London					Glasgow			
	Easting Coeff	Northing Coeff	P-value	R^2		Easting Coeff	Northing Coeff	P-value	R^2
Site 1	-8.051e-06	1.637e-05	0.997	<0.10	Site 1	7.294e-05	7.753e-05	0.968	<0.10
Site 2	-0.0008	0.001	0.0001	0.45	Site 2	0.0003	0.0002	0.861	<0.10
Site 3	-0.0002	-0.0003	0.230	0.08	Site 3	-0.0009	-0.0006	0.092	0.29
Site 4	-4.836e-05	9.345e-05	0.794	<0.10	Site 4	9.095e-06	-0.0009	0.055	0.19
Site 5	-3.351e-05	0.0002	0.038	0.15	Site 5	-0.0005	0.0001	0.444	0.04
Site 6	0.0001	-9.128e-05	0.367	0.07	Site 6	0.0006	0.0006	0.410	0.07
Site 7	0.001	0.002	0.060	0.26	Site 7	-2.459e-05	6.853e-05	0.956	<0.10
Site 8	-6.082e-05	2.948e-05	0.923	<0.10	Site 8	0.0007	-0.0002	0.132	0.21

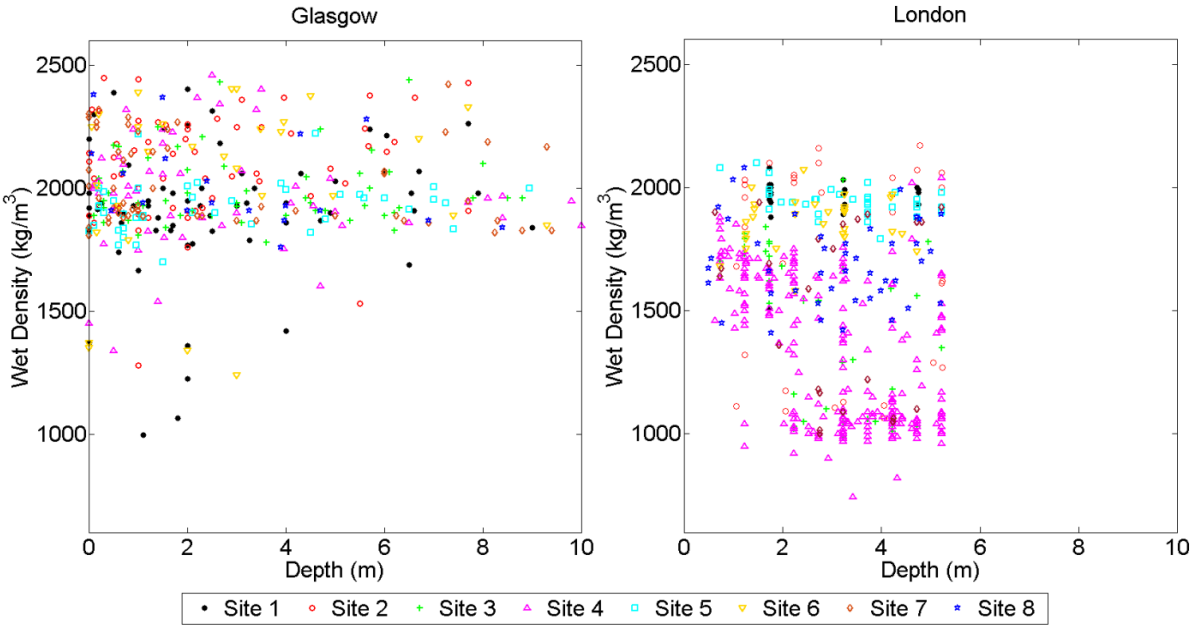

Figure 6: The relationship between the wet bulk density of the soil and depth for the 8 Glasgow and 8 London clusters of borehole records. No clear correlations indicating a relationship with depth were visible for any of the measured sites with the exception of London site 4. The results of regression for these sites are shown in Table 3.

Table 3: Attempted linear regression between depth and density for all of the study sites

London			Glasgow		
	Coefficient Estimate	P value		Coefficient Estimate	P value
Site 1	-0.007	0.711	Site 1	-0.009	0.439
Site 2	-0.035	0.549	Site 2	-0.004	0.518
Site 3	0.012	0.496	Site 3	0.022	0.387
Site 4	-0.024	0.0008	Site 4	0.010	0.091
Site 5	-0.115	0. 461	Site 5	-0.003	0.761
Site 6	-0.124	0.184	Site 6	-0.003	0.598
Site 7	-0.006	0.894	Site 7	0.011	0.228
Site 8	0.008	0.596	Site 8	0.014	0.168

3.3. Summary of Desk Study Findings

The main implications for the modelling from the findings of this desk based study are as follows:

- Density variation is in the range of between 300 kg/m^3 and 1500 kg/m^3 but typically around 600 kg/m^3 to 900 kg/m^3. A density range within these boundaries is reasonable and justified for modelling the effects of variation of the near surface density on gravity and gravity gradient measurements in the next section based on the data studied here, although the relationship between this parameter and the overall soil noise should also be investigated in case other potential survey areas fall outside this range.
- The precise wavelength of the density variation was difficult to determine due to the available borehole data being a few metres apart even for the closest spaced boreholes. However, it is almost certain that the wavelength of density variation is smaller than the scale of measurement spacing between boreholes so the modelling should focus on a range of density wavelengths shorter than a few metres.
- Density variation appears to be randomly distributed rather than periodic or following the underlying trends in soil type and geology. The density values were normally distributed, although some of the sample sizes were small making them appear to look like bimodal distributions or distributions which do not fit any standard models of distribution, but appear to be between normal and uniform distributions. Modelling both normal and uniform distributions

should encompass the range of soil noise effect that might be present, allowing the effects to be quantified and characterised.

4. Computer Simulation of Soil Noise

4.1. Method

The nature of near surface density variations are used to build models to understand the implications of these variations on gravity and gravity gradient measurements. The variation of density in the subsurface can be modelled as a 3 dimensional matrix of discrete cells, with densities either randomly or systematically assigned. These can be represented by simple geometric shapes such as spheres or cubes (parallelepipeds). Of these, spheres have the advantage of being computationally less expensive, and preliminary testing showed similar results between the two shapes, providing the height of the sensor is greater than the sphere radius or cube side length, as is the case in the current work. The vertical gravity of a sphere for a given point above the ground surface is given by Equation 1 (Telford, Geldart and Sheriff, 1990).

$$g_{sphere} = \frac{4\pi G\rho R^3}{3}\frac{z}{(x^2+z^2)^{3/2}} \quad [1]$$

Where G is the gravitational constant, ρ is the density contrast of the sphere in kg/m^3, R is the radius of the sphere in m, and x and z are the horizontal and vertical distances (+ve down) to the centre of the sphere in m respectively. This equation was used to create a suite of computer simulated forward models in MATLAB®, which were used to model the near surface density variations as a 3-dimensional matrix of spheres (radius = 0.05 m) with varying density (Figure 7). The dimensions of the model were X =

100 m, Y = 100 m, with the Z parameter tested at 0.25, 0.5, 1 and 2 m in order to test the effects of soil thickness on the observed results. The gravity was calculated along a 50 m long line of observation points, with a measurement spacing of 0.1 m, and at a range of different heights (0.25, 0.5, 0.75, 1.00 and 2.00 m), allowing the effects of varying the height of the sensor and gradiometer separation to be investigated by calculating the difference in gravity between different pairs of vertically separated points.

Although the desk study identified that the density varied on a spatial scale smaller than the spacing of the closest spaced borehole data (i.e. within a few metres), the precise wavelength of density variations could not be determined. This spatial wavelength of density variation is an important factor to consider because shorter wavelengths have both relatively high and low density soil cells in close proximity, creating an almost equal positive and negative contribution to the measured value for any given point. This produces smaller amplitude variations which are also at shorter signal wavelengths than signals from buried features and therefore easier to distinguish from these signals. In contrast, longer wavelengths of density variations are more likely to produce gravity signals which are of a similar signal wavelength and likely to be mistaken for target features of interest. The spatial wavelength at which density variations drop to an insignificant level is also dependent on the instrument configuration, especially in terms of the sensor height and, in the case of a gravity gradiometer instrument, the separation between the two sensors.

Thus, three different types of modelling were used to assign density values to the spheres to assess the consequences of different wavelengths of density variation and density distributions. For all the modelling, spheres were grouped into cubes with side lengths of 0.1 m, 0.2 m, 0.4 m and 0.8 m (i.e. 1, 2, 4 and 8 spheres) to look at the effects of different spatial scales of density variation within the range identified by the desk study. Ten simulations were run for each side length. The three different model types were:

1. Density of the spheres determined using random draws of densities from a normal distribution (Figure 7a) representing sites which were approximated by this density distribution (see desk study). The density range was approximated as being equal to three standard deviations.
2. Density of the spheres determined using random draws of densities from a uniform distribution (Figure 7a). This represents the worst case scenario for soil noise.
3. Periodic density variation using sinusoidal distributions of density in the X direction with wavelengths of density variation between 0.4 and 2 m (Figure 7b). This provided a systematic approach to identify the relationship between different wavelengths of density variation and the resulting soil noise, and allowed some rules of thumb to be developed for the noise as a function of sensor configuration in terms of height and sensor separation.

The density variation range used was 800 kg/m^3 which is the median value observed within the desk study and therefore within the range of observed density variations

identified for the sites used (between 300 kg/m^3 and 1500 kg/m^3) as well as being close to the average of 850 kg/m^3. However, additional testing, showed that for both gravity and gravity gradient signals, the magnitude of the soil noise scales linearly with the density range, regardless of the wavelength of density variation and depth of soil, and the observed trends with sensor height and separation are unchanged. Some example results of this testing are shown in Figure 8 for gravity (Figure 8a) and gravity gradient signals (Figure 8b).

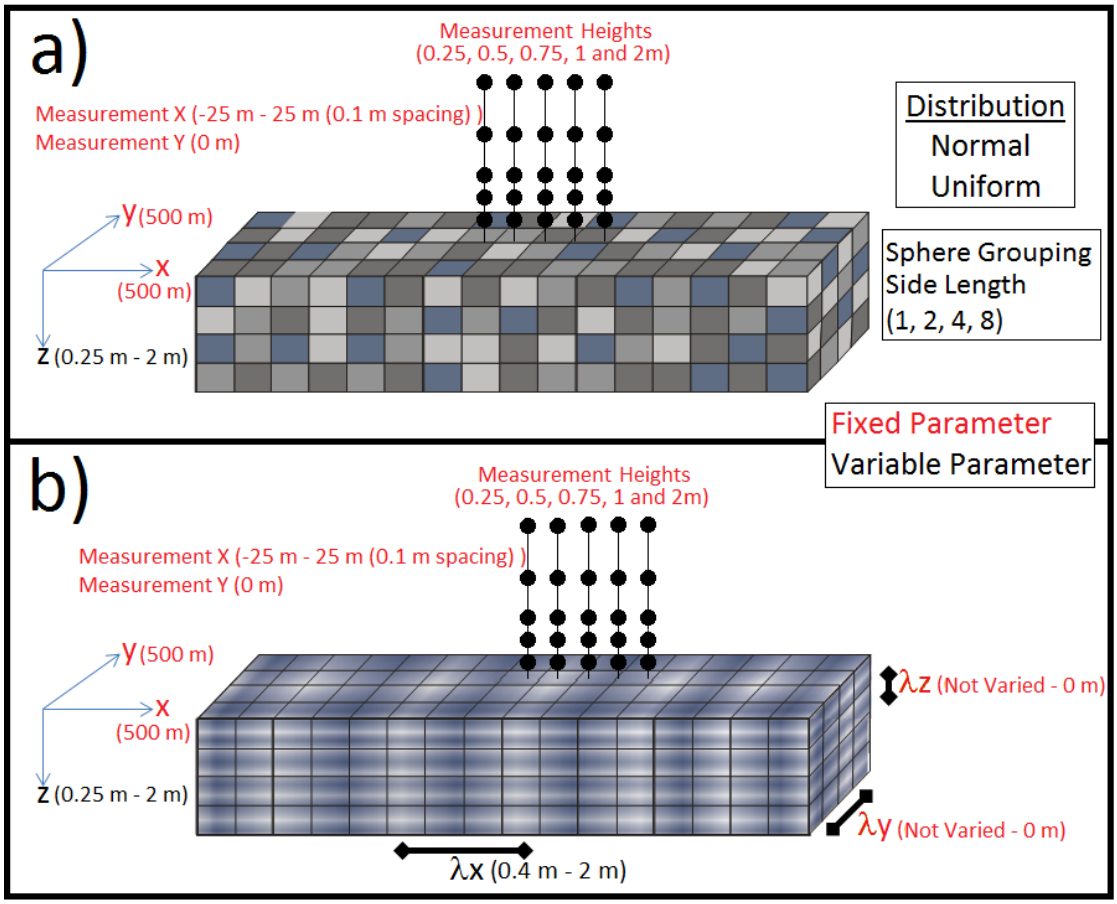

Figure 7: Schematic representation of modelling methods including fixed and variable parameters a) Using a random distribution and b) using a periodic model

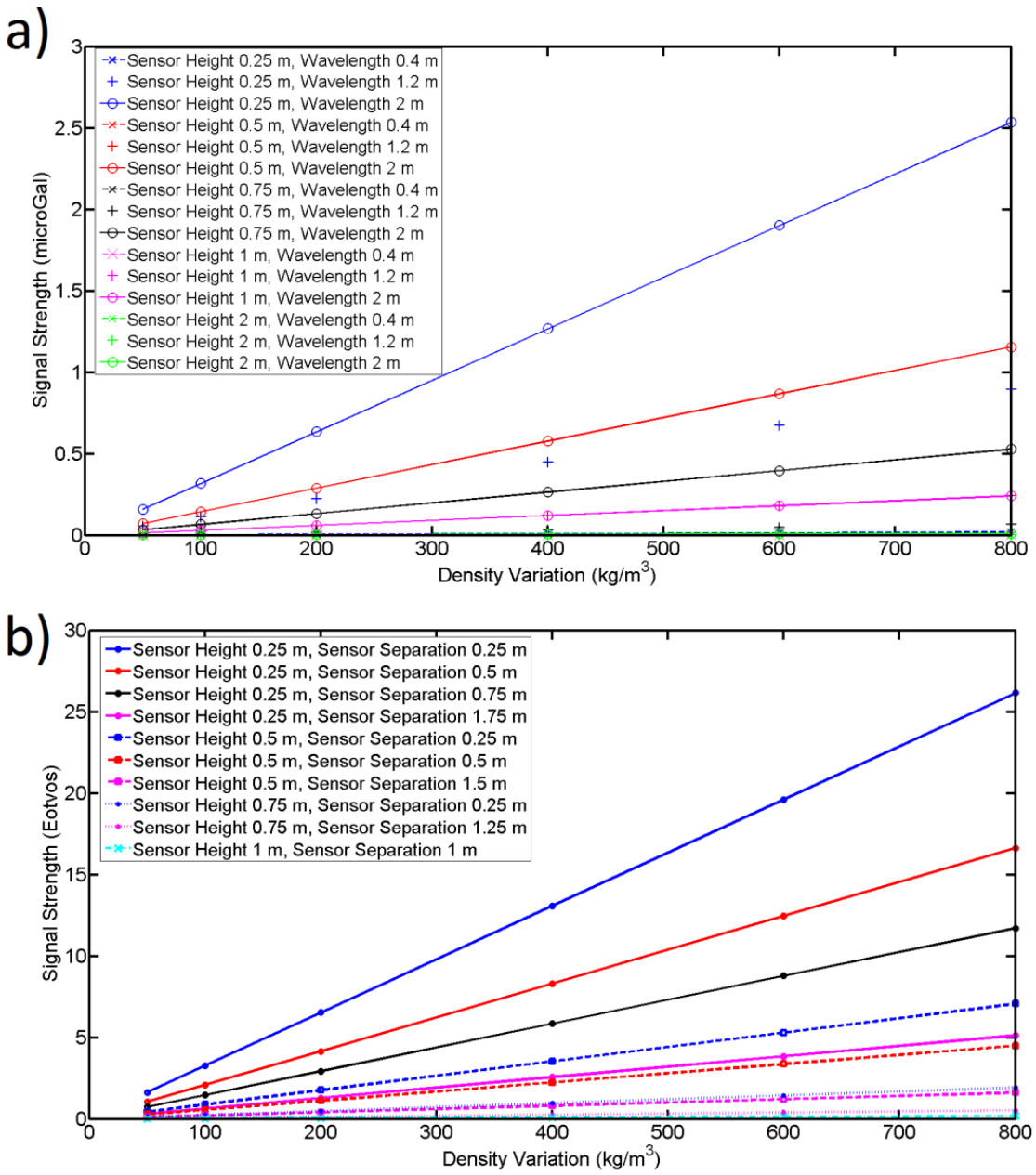

Figure 8: The effects of varying the density range on measured soil noise and the linear trends between the two for a given sensor configuration a) The effects on gravity measurements and b) the effects on gradiometer measurements for a 1.2 m periodically varying density

3.2. Effects on Gravity Signals

The results of the periodic variation simulations were used to identify the behaviour of the soil noise in a tightly controlled parameter space and identify the relationships

between different variation length scales and sensor configurations. Maximum signal strength has been identified by subtracting the minimum value from the maximum value in each simulation to quantify the scale of the noise on gravity data. The results of these simulations on measured gravity data, and the relationship between the wavelength of density variation, depth and sensor height are shown in Figure 9. However, as evidenced by the desk study, density variation does not typically follow periodic trends but varies randomly. The results of the simulations with the more realistic random density variation models on gravity readings are shown in Figure 10 for both normal and uniform distributions. Results from ten different simulations for each scenario have been averaged, and the standard deviation used to generate error bars which represent the effects of variations in the density distribution.

As expected, analysis of the periodic density model (Figure 9) shows that regardless of the wavelength of density variation and soil depth, the soil noise peaks when the sensor is closest to the ground (0.25 m), with a maximum value of 2.53 μGal (soil depth 2.0 m, wavelength 2.0 m). The random density distributions (Figure 10) also showed similar trends, with maximum values of 2.92 μGal for normal distributions of density and 4.79 μGal for uniform distributions of density respectively (both 0.8 m cube side lengths). All of these values are well under the typical repeatability of current spring based field microgravity instruments (typically ±5 μGal), which highlights why this noise is both difficult to currently quantify and not generally considered in current surveys. Nevertheless, the noise has the potential to affect more sensitive gravimeter instruments such as those under development based on quantum technology (e.g. Freier et al., 2016; Muquans, 2017). However, the practical resolution of these devices

will be affected by environmental vibrational noise (e.g. from microseisms) and will require sufficiently long integration times for each measurement point in order to reach an accuracy and precision level comparable to this noise.

The noise also increases as the depth of the soil containing density variation is increased. However for periodic variations in density with wavelengths of density variation between 0.4 m and 2 m, beyond 1 m depth the observed increases are almost negligible (increases are < 0.1 μGal for all tested examples). The same effect can also be seen for random variations in density. Although the rate at which it increases is slightly greater for the uniform distribution, as with the periodic distribution the effect is very small in all scenarios, with differences of less than 0.5 μGal noted between 1 and 2 m soil depth in the worst case scenario (uniform distribution, instrument height 0.25 m). This would suggest that only the first metre has a substantial impact on the measured noise above the practical resolution of existing instruments. Both periodic density variations (Figure 9) and random variation simulations (Figure 10) show that the noise also increases with increasing wavelength of the density variation or cube size. For small soil depths, this relationship is linear although for greater soil depths, this tends towards a quadratic relationship. The distribution of density is also an important factor and random noise with a uniform distribution of density is roughly 40% - 50% higher than the noise generated by normal distributions for the same soil thickness and soil unit size.

In terms of the configuration, the soil noise is supressed rapidly with increasing height of the gravimeter above the ground surface due to the increase in distance from the

causative bodies. For periodic density variation, at heights of 0.5 m and above the resulting noise is below the resolution of current gravimeter instruments (1 μGal for the CG-5) for all of the tested configurations and far below the repeatable practical resolution. These values continue to drop off to below 0.5 μGal for a height of 0.75 m, 0.25 μGal for 1 m height and 0.12 μGal for 2 m height. Increasing the height of the sensor also decreases the amplitude of the noise from the soil variations, and increases the wavelength spectrum of the signal observed. For example, at a height of 0.5 m above the ground, wavelengths of soil density variation up to 1 m produce very small gravity responses which are unlikely to be detected (< 0.25 μGal), whereas at 0.75 m height, wavelengths of density variation up to 1.6 m fall under this threshold. At heights of 1 m and above, only very small differences (< 0.25 μGal) can be seen regardless of the wavelength of density variation within the tested range (up to 2 m). Similar relationships were observed for the randomly varying soil density models, although unlike with periodic variation simulations, the stochastic effects mean that no height was observed at which the scale of the noise (defined as the range of the amplitude) could be guaranteed to fall below the practical resolution of current instruments. However at 2 m, all but the uniform distribution with the 0.8 m side lengths (i.e. the worst case scenario) fall below 1 μGal. It should be recognised that the improvement caused by offsetting the soil noise in this way must be balanced against the subsequent decrease in the signal from the targets of interest as this will be further away. It should also be considered that gravimeter instruments are more strongly affected by vibrational noise from microseisms and anthropogenic activity in the surrounding area which require lengthy integration times to average out. Given

the small signal strengths in all of the tested scenarios and the length of time required to reach an appropriate level of precision, it is unlikely that soil noise will be the limiting factor for future commercial gravimeter surveys, even using QT gravimeter sensors.

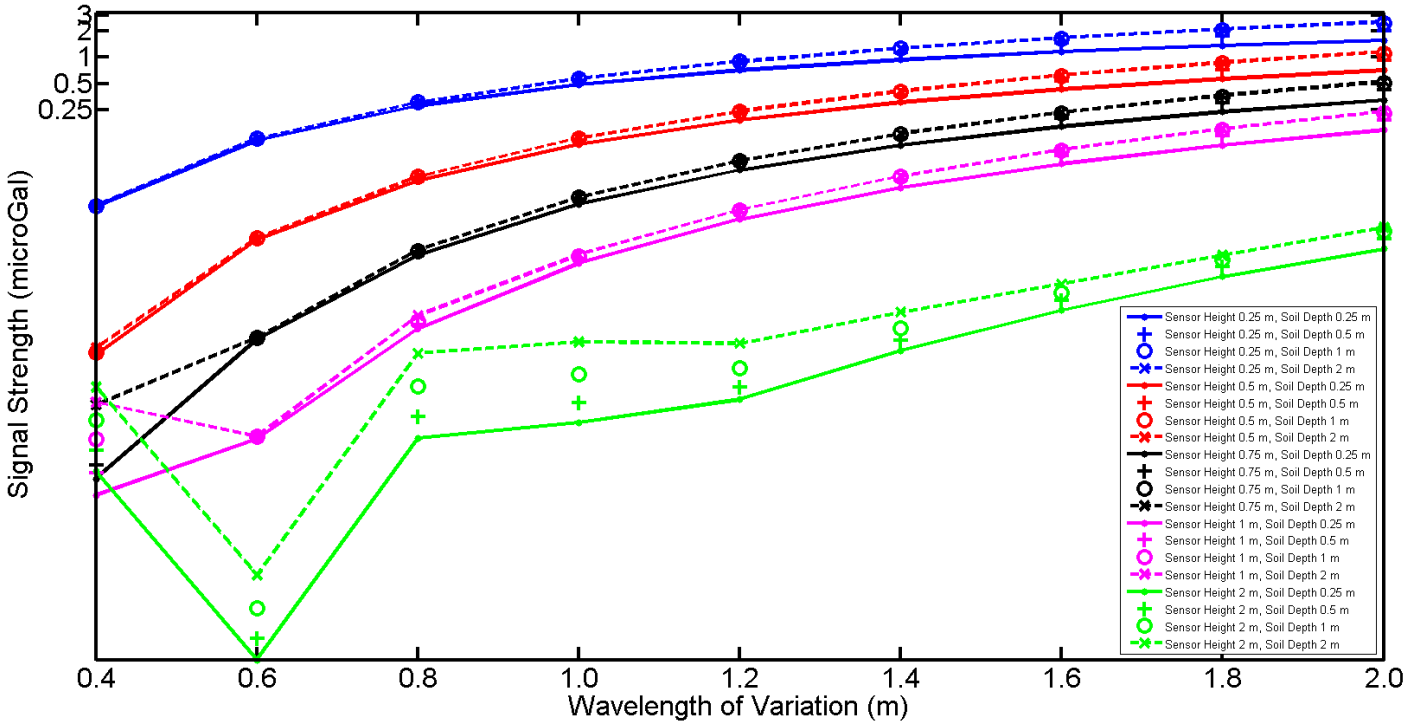

Figure 9: The relationship between wavelength of periodic density variation, depth of the soil, sensor height and signal strength of the soil

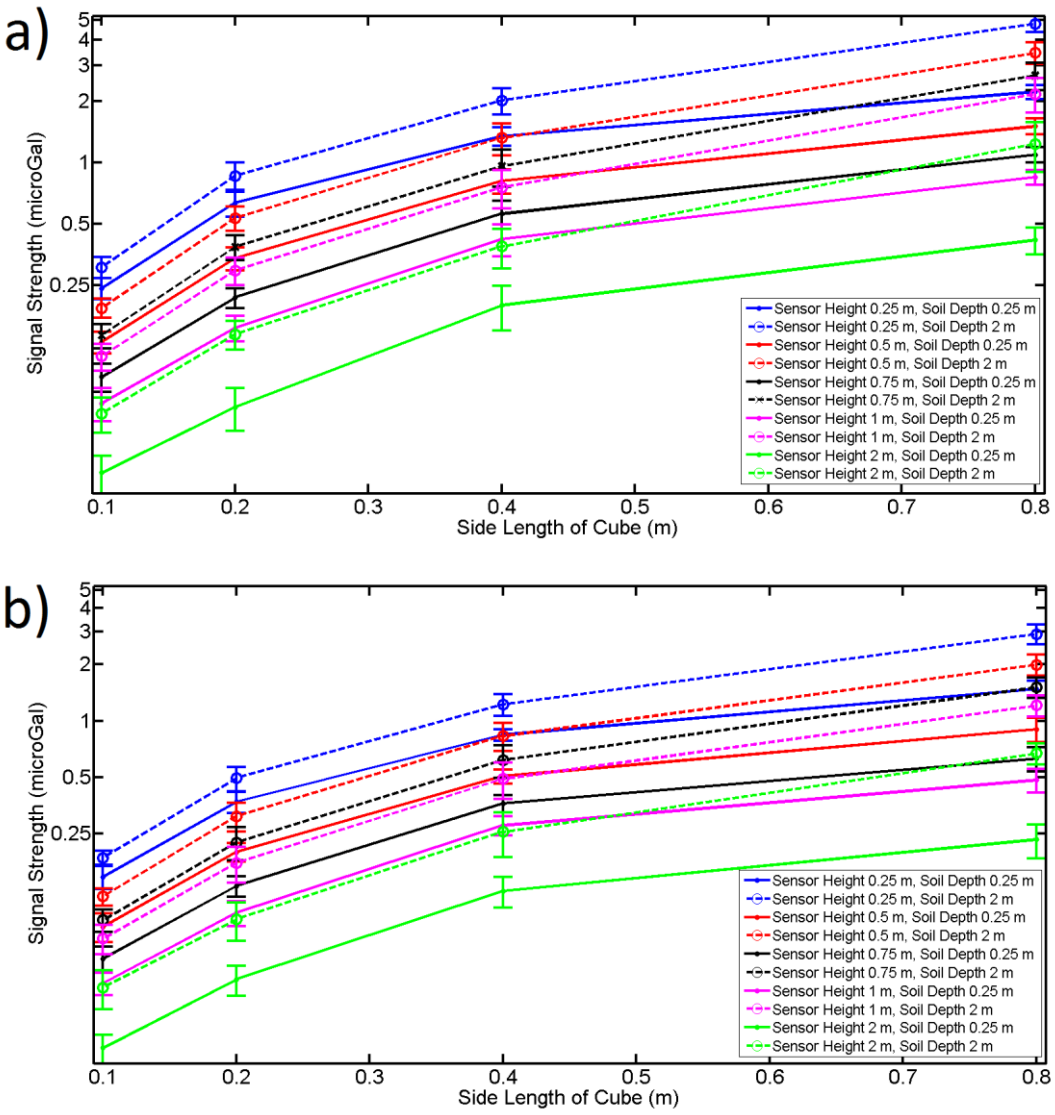

Figure 10 Effects of different side lengths and soil thickness for a) a uniform distribution and b) a normal distribution

3.3. Effects on Gravity Gradient Signals

Due to their ability to strongly suppress environmental noise effects, it is expected that the use of gradiometers for field surveys is more likely in the future due to the promised increase in speed, accuracy and precision of the measurements (Boddice, Metje and Tuckwell, 2016; Boddice et al., 2017; Hinton et al., 2017). The effects of soil

noise on gradiometer readings have been assessed by using simulated gravity at two different heights and Equation 2.

$$g_{zz} = \frac{\left(g_{z(bottom)} - g_{z(top)}\right)}{z_{sensor}} \quad [2]$$

Where g_{zz} is the instrument recorded gravity gradient, g_z is the gravity recorded at different heights and z_{sensor} is the height difference between the two gravity measurements in metres (i.e. height of the top sensor – height of the bottom sensor).

Calculation using a range of possible combinations of the simulated gravity data at different heights above the ground allows the effects of sensor heights and separations to be investigated by generating different gradiometer configurations. The relationships between the soil noise, soil depth and sensor height for a gradiometer with a 0.25 m separation between the top and bottom sensors for a range of different wavelength periodic distributions of gravity is shown in Figure 11. The broad trends are similar to those observed with the gravity noise, although, unlike with the gravity noise and as expected, the noise generated by soil is almost always in the range that would be considered significant (> 1 Eötvos) due to the derivative calculation which biases measurements to nearby sources. Based on the information gained from the desk study, more realistic survey scenarios can again be analysed by looking at the data generated using random rather than periodic density variations. The effects of random density variations for both uniform and normal density distributions for gravity gradiometers with a 0.25 m separation between the two atom clouds is shown in Figure 12. As with the noise generated for periodic density variation, the noise

generated by soil is almost always in the range that would be considered significant (i.e. > 1 Eötvos).

Much as with the gravimeter, increasing the depth of the soil containing density variation causes the noise to increase. For increases in soil depth beyond 1 m, these effects are small, with the differences in observed noise effects between 1 and 2 m soil depths less than 3 Eötvos for all tested examples. However, as proposed gradiometer instruments could have a resolution of 1 Eötvos, and 3 Eötvos is comparable to the maximum signal from typical civil engineering targets such as pipes and small solution features, this increase could be considered significant for surveying purposes, unlike the increases in gravity seen for a similar increase in soil depth. As with the gravity soil noise, the gradient signal from the soil noise also increases as the wavelength of density variation increases for the periodic variation model (Figure 11) or cube side length (Figure 12) for the random density variation model. However, unlike the gravity signal, this increase is not linear, but a function of the soil depth. The rate at which the soil noise increases with increasing wavelength of density variation is not only much less for the 0.25 m and 0.5 m thick soils in comparison to the 1.0 m and 2.0 m thick soils, but also slows as the wavelength of density variation increases, seen as the curve flattens at wavelengths above 1.4 m in Figure 11 and cube lengths of 0.8 m in Figure 12. For random density models, the increase in soil noise with increasing soil cube side length is also less pronounced at higher side lengths for the uniform distribution in comparison to the normal distribution, especially for shallow soil depths. Interestingly, this trend is the opposite to those observed for the gravity signals where the uniform

density distribution gave a large rate of noise increase with increasing side length of the cubes.

As with the gravimeter instrument, increasing the height of the sensor supresses the noise, although it must also be recognised that the improvement caused by offsetting the soil noise in this way must be balanced against the subsequent decrease in the signal from the targets of interest which will be more significant with gravity gradient measurements which decrease at a greater rate with distance from the target (for point sources and spherical features for example, the signal decreases at a rate of $1/z^3$ for gravity gradients as opposed to only $1/z^2$ for gravity signals). The optimum height for the purposes of surveying using a gradiometer instrument will be determined by the optimisation between using the instrument at a greater height to supress noise and leaving the instrument close to the ground to maximise signals from targets of interest. Soil noise can also be suppressed by increasing the separation between the top and bottom sensors which causes the instrument to become relatively more sensitive to deeper sources, which may be more beneficial than changing the height of the instrument as it does not weaken the signal from the target of interest as severely. The effects of changing the sensor separation are shown in Figure 13 for periodic density distribution and Figure 14 for random density distributions. This shows that this is less effective at supressing the soil noise than changing the height of the sensor. For example for a 2 m thick layer of soil with uniform random distribution with a side length of 0.4 m, increasing the sensor separation of an instrument at 0.25 m above the ground from 0.25 to 0.5 m decreases the noise by 8 Eötvos compared to a decrease of 16 Eötvos from lifting the whole instrument from 0.25 m to 0.5 m. A similar plot for

normal distributed noise shows noise reduction of 5 and 10 Eötvos for the same criteria. A similar result is also observed for a change in height from 0.5 m to 0.75 m and an increase in sensor separation from 0.25 m to 0.5 m (2 and 4 Eötvos respectively).

Therefore it appears that increasing the instrument separation by the same distance is only 50% as effective as increasing the height of the whole instrument. Nevertheless, increasing the separation may provide a more practical solution towards suppressing the soil noise for two main reasons; first, lifting the whole instrument off the ground may prove impractical for field deployment due to the expected weight of the first generation of QT gravity gradient instruments and difficulty in designing an appropriate system to carry the instrument. Secondly, and perhaps more crucially, measuring with a small separation requires far greater sensitivity and low noise characteristics to be achieved by the sensor head due to the smaller difference in the gravity signals between the top and bottom sensor which may be beyond the technological limitations of the instrument's design.

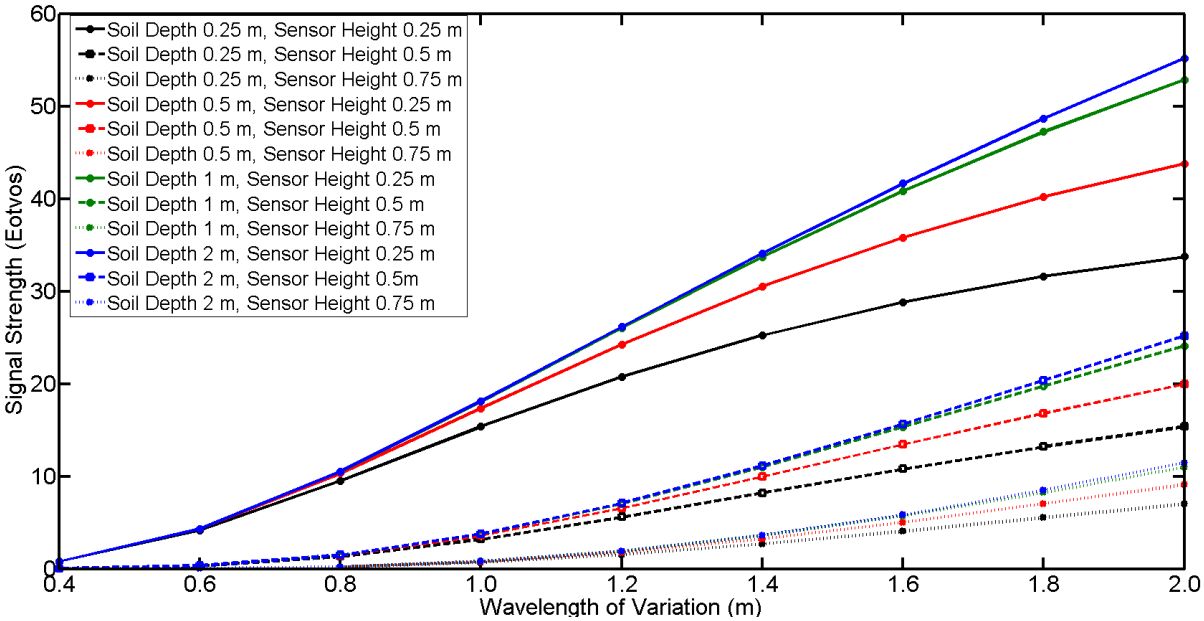

Figure 11: Effects of Soil Depth and Sensor height for a 0.25 m gradiometer

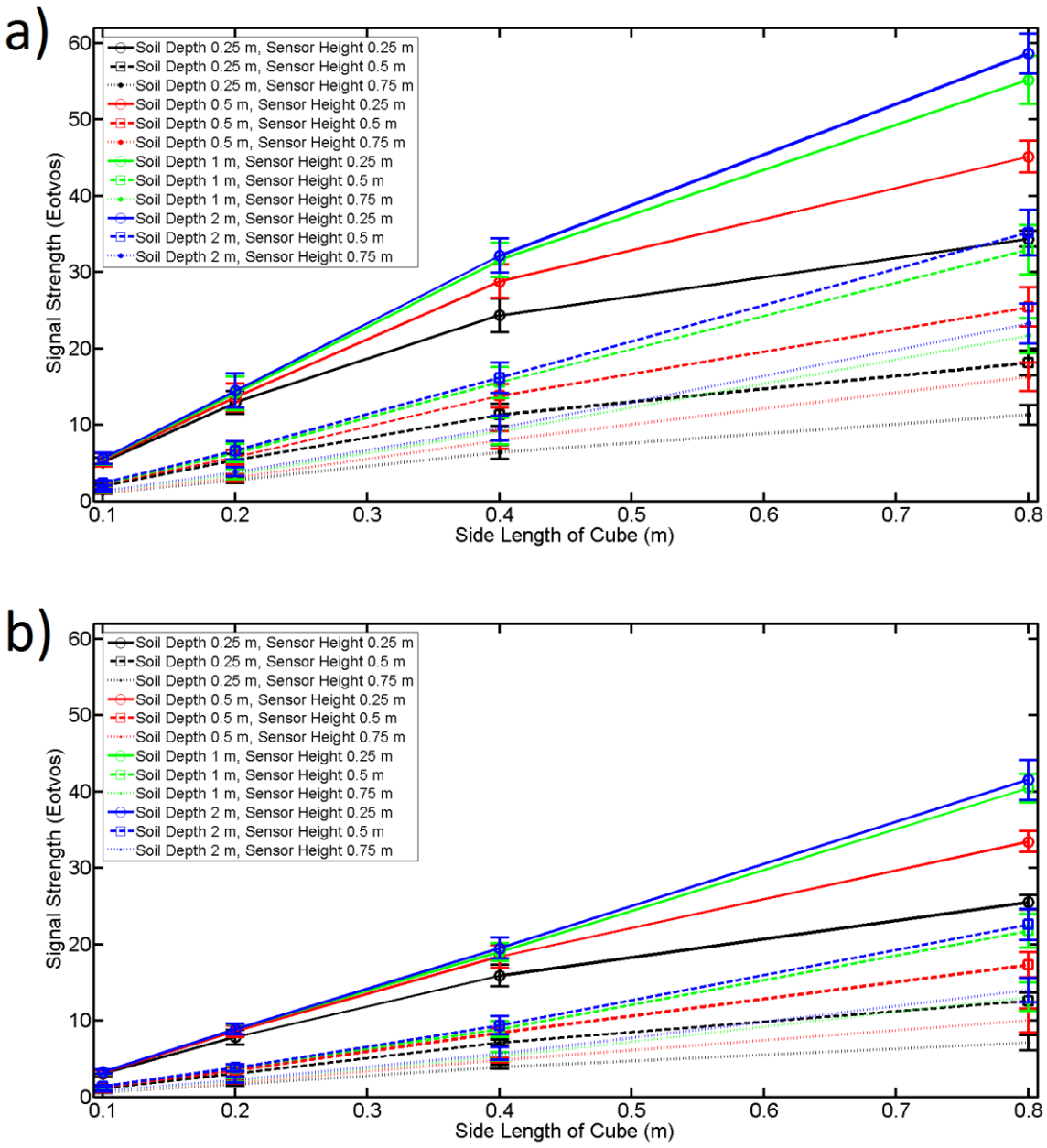

Figure 12: Effects of Soil Depth and Sensor height for a 0.25 m gradiometer for a) a uniform distribution and b) a normal distribution

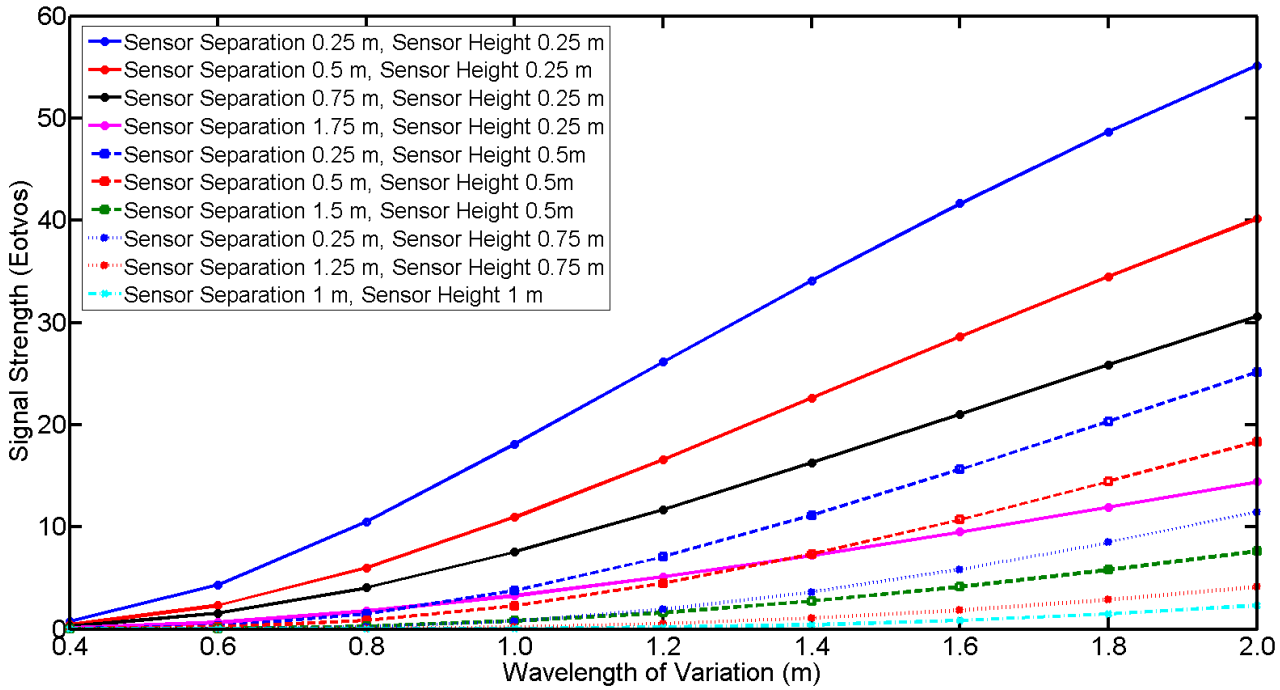

Figure 13: Effects of Sensor separation and sensor height on a 2 m thick soil layer with periodic density variation

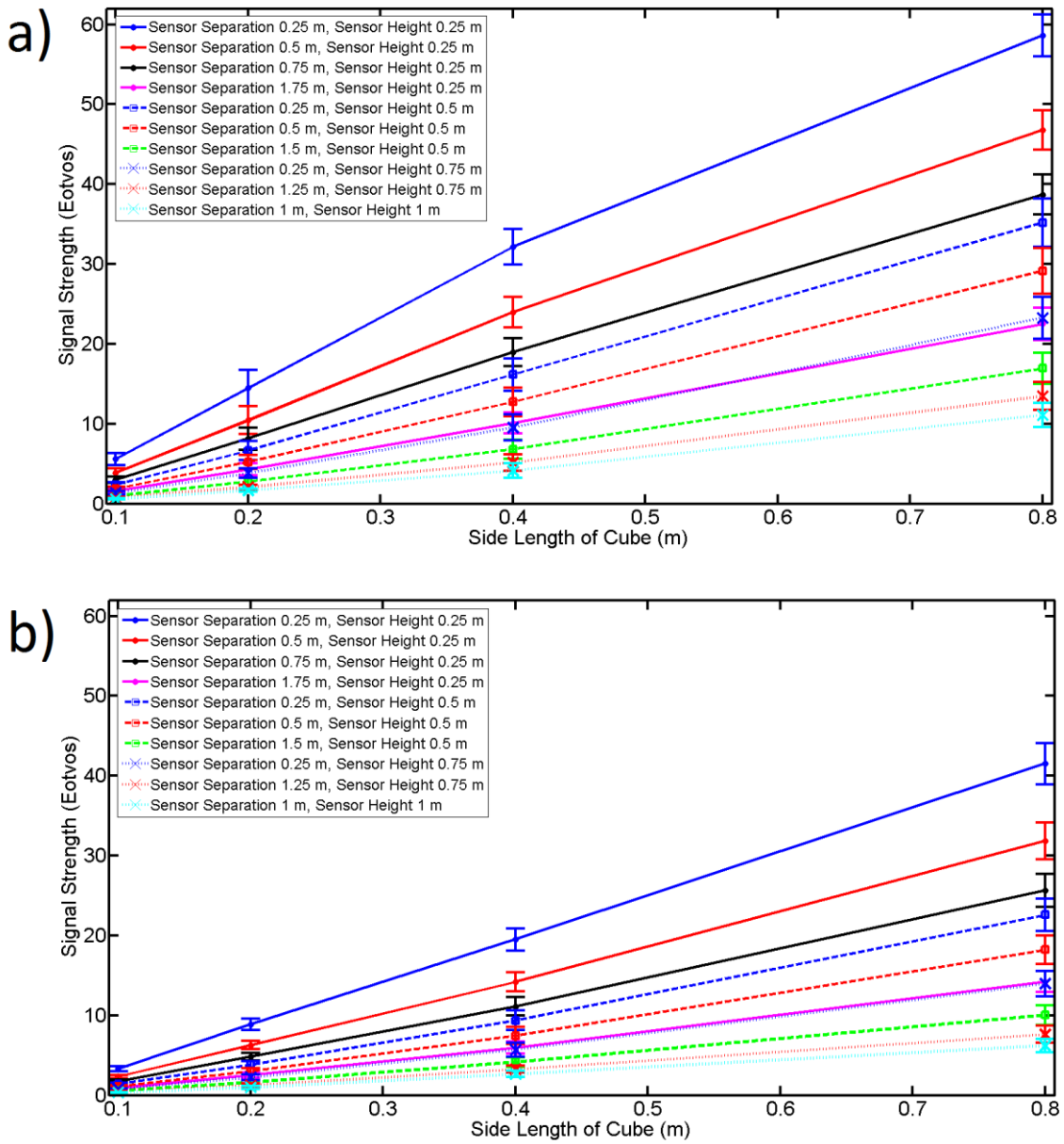

Figure 14: Effects of Sensor separation and sensor height on a 2 m thick soil layer with random density variation for a) a normal distribution and b) a uniform distribution

3.4. Practical effects of soil noise on gradiometer readings for different targets

As demonstrated above, the noise from near surface density variation can be mitigated by either increasing the height of the instrument above the ground or the separation between the top and bottom sensor. However, it should be recognised that either of these methods will also reduce the desirable signal from the buried target of interest. The configuration of a gravity gradient instrument for surveying purposes will be determined by the optimisation between using the instrument at a greater height to supress noise and leaving the instrument close to the ground to maximise signals from targets of interest. Increasing the height of the sensor also has the effect of increasing the spatial signal wavelength of the soil noise, which may take it into a range closer to the signal wavelength of buried targets. This may be undesirable as noise within a different spatial range can be suppressed using spatial filtering techniques to enhance the features of interest. Another consideration is the required sensitivity of the new instrument for a given configuration. Since QT instruments work by detecting the difference in gravity between two atom clouds and converting these values to gravity gradient values, closely spaced separations between the top and bottom sensors require much greater sensitivity in order to be able to detect the difference in gravity even though the gravity gradient may be stronger.

In order to give a realistic assessment of the limitations on detection of buried features created by soil noise, it is necessary to consider three main factors: the amplitude of the noise in relation to the signal strength from the target of interest, the required

sensitivity of the instrument, and the comparative signal wavelengths of the noise and relevant anomaly. To indicate how the identified soil noise may affect the outcome of a typical geophysical survey, spherical voids, which represent a typical underground risk to civil engineering projects, have been modelled using spheres of different radii between 0.5 and 2 m and depths between 2 and 15 m using Equation 1. The anomaly widths (calculated using the width between zero crossing points of the anomaly) for different depth targets measured using the same range of configurations to determine the soil noise are shown in Table 4. The main factor for determining the signal wavelength is the depth of the buried target and overall height of the instrument (i.e. the distance from the target), with the instrument separation also having a contributory effect. In contrast, the radius of the sphere had no effect on the signal wavelength, with identical results for spheres of 0.5 m and 2 m radii (not shown). The signal strengths for the same data are displayed in Table 5 with the size of the buried feature being the greatest factor in determining the signal size, followed by the distance from the object (i.e. object depth and height of the sensor). Increasing the sensor separation also causes the signal to decrease, albeit with a less pronounced effect than increasing the instrument height. For example, changing the instrument separation from 0.25 m to 0.5 m produces a 50% smaller percentage change in the signal size. This can be seen in Figure 15.

Table 4: The anomaly widths in m for a 1 m spherical void at different depths for a range of gradiometer configurations

Target Depth (m)	Sensor Height (m)		Sensor Separation (m)							
			0.25	0.5	0.75	1	1.25	1.5	1.75	2
2	Sensor Height (m)	0.25	6.8	7	7.4	7.6	8	8.2	8.6	8.8
		0.5	7.4	7.8	8	8.4	8.8	9	9.2	
		0.75	8.2	8.4	8.8	9.2	9.4	9.8		
		1	8.8	9.2	9.6	9.8	10.2			
		1.25	9.6	9.8	10.2	10.6				
		1.5	10.2	10.6	11					
		1.75	11	11.2						
		2	11.6							
5	Sensor Height (m)	0.25	7.4	15.6	15.8	16.2	16.6	16.8	17.2	17.6
		0.5	16	16.2	16.6	17	17.2	17.6	17.8	
		0.75	16.6	17	17.4	17.6	18	18.2		
		1	17.4	17.6	18	18.4	18.6			
		1.25	18	18.4	18.8	19				
		1.5	18.8	19	19.4					
		1.75	19.4	19.8						
		2	20.2							
10	Sensor Height (m)	0.25	29.4	29.6	30	30.4	30.8	31	31.4	31.8
		0.5	30	30.4	30.8	31	31.4	31.8	32.2	
		0.75	30.8	31.2	31.4	31.8	32.2	32.4		
		1	31.4	31.8	32.2	32.6	32.8			
		1.25	32.2	32.6	32.8	33.2				
		1.5	32.8	33.2	33.6					
		1.75	33.6	34						
		2	34.2							
15	Sensor Height (m)	0.25	43.4	43.8	44.2	44.6	44.8	45.2	45.6	45.8
		0.5	44.2	44.6	44.8	45.2	45.6	46	46.2	
		0.75	45	45.2	45.6	46	46.2	46.6		
		1	45.6	46	46.4	46.6	47			
		1.25	46.4	46.6	47	47.4				
		1.5	47	47.4	47.8					
		1.75	47.8	48						
		2	48.4							

Table 5: The signal strengths in Eötvos for different size and depth targets for a range of gradiometer configurations.

Target Depth (m)		Sensor Height (m)	Target Radius (m) = 0.5 / Sensor Separation (m) = 0.25	0.5	0.75	1	1.25	1.5	1.75	2
2		0.25	9.1	7.9	7.0	6.2	5.6	5.1	4.7	4.3
		0.5	6.7	5.9	5.3	4.7	4.3	3.9	3.6	
		0.75	5.1	4.5	4.1	3.7	3.4	3.1		
		1	4.0	3.6	3.2	2.9	2.7			
		1.25	3.2	2.8	2.6	2.4				
		1.5	2.5	2.3	2.1					
		1.75	2.1	1.9						
		2	1.7							
5		0.25	6.7	0.7	0.7	0.6	0.6	0.6	0.5	0.5
		0.5	0.7	0.6	0.6	0.6	0.5	0.5	0.5	
		0.75	0.6	0.6	0.5	0.5	0.5	0.5		
		1	0.5	0.5	0.5	0.4	0.4			
		1.25	0.5	0.4	0.4	0.4				
		1.5	0.4	0.4	0.4					
		1.75	0.4	0.4						
		2	0.3							
10		0.25	0.11	0.10	0.10	0.10	0.09	0.09	0.09	0.09
		0.5	0.10	0.10	0.09	0.09	0.09	0.09	0.08	
		0.75	0.09	0.09	0.09	0.09	0.08	0.08		
		1	0.09	0.09	0.08	0.08	0.08			
		1.25	0.08	0.08	0.08	0.07				
		1.5	0.08	0.07	0.07					
		1.75	0.07	0.07						
		2	0.07							
15		0.25	0.03	0.03	0.03	0.03	0.03	0.03	0.03	0.03
		0.5	0.03	0.03	0.03	0.03	0.03	0.03	0.03	
		0.75	0.03	0.03	0.03	0.03	0.03	0.03		
		1	0.03	0.03	0.03	0.03	0.03			
		1.25	0.03	0.03	0.03	0.03				
		1.5	0.03	0.03	0.03					
		1.75	0.03	0.02						
		2	0.02							

Target Depth (m)		Sensor Height (m)	Target Radius (m) = 1 / Sensor Separation (m) = 0.25	0.5	0.75	1	1.25	1.5	1.75	2
2		0.25	72.6	63.2	55.7	49.7	44.8	40.7	37.2	34.3
		0.5	53.7	47.3	42.1	37.9	34.4	31.4	28.9	
		0.75	40.9	36.3	32.6	29.5	27.0	24.8		
		1	31.8	28.5	25.8	23.5	21.6			
		1.25	25.2	22.8	20.7	19.0				
		1.5	20.4	18.5	16.9					
		1.75	16.7	15.2						
		2	13.8							
5		0.25	53.7	5.8	5.5	5.2	4.9	4.6	4.4	4.2
		0.5	5.4	5.1	4.8	4.5	4.3	4.1	3.9	
		0.75	4.8	4.5	4.2	4.0	3.8	3.6		
		1	4.2	4.0	3.8	3.6	3.4			
		1.25	3.7	3.5	3.3	3.2				
		1.5	3.3	3.2	3.0					
		1.75	3.0	2.8						
		2	2.7							
10		0.25	0.9	0.8	0.8	0.1	0.8	0.7	0.7	0.7
		0.5	0.8	0.8	0.8	0.1	0.7	0.7	0.7	
		0.75	0.8	0.7	0.7	0.1	0.7	0.6		
		1	0.7	0.7	0.7	0.1	0.6			
		1.25	0.7	0.6	0.6	0.1				
		1.5	0.6	0.6	0.6					
		1.75	0.6	0.6						
		2	0.5							
15		0.25	0.3	0.3	0.3	0.2	0.2	0.2	0.2	0.2
		0.5	0.3	0.2	0.2	0.2	0.2	0.2	0.2	
		0.75	0.2	0.2	0.2	0.2	0.2	0.2		
		1	0.2	0.2	0.2	0.2	0.2			
		1.25	0.2	0.2	0.2	0.2				
		1.5	0.2	0.2	0.2					
		1.75	0.2	0.2						
		2	0.2							

Target Depth (m)		Sensor Height (m)	Target Radius (m) = 2 / Sensor Separation (m) = 0.25	0.5	0.75	1	1.25	1.5	1.75	2
2		0.25	580.9	505.3	445.7	397.7	358.3	325.6	298.0	274.4
		0.5	429.8	378.3	336.9	303.0	274.9	251.2	231.0	
		0.75	326.9	290.6	261.0	236.4	215.7	198.1		
		1	254.4	228.1	206.3	188.0	172.4			
		1.25	201.9	182.4	166.0	152.1				
		1.5	162.9	148.1	135.5					
		1.75	133.3	121.9						
		2	110.5							
5		0.25	429.8	46.7	43.9	41.3	39.0	37.0	35.1	33.4
		0.5	43.5	40.9	38.5	36.3	34.4	32.6	31.0	
		0.75	38.2	36.0	33.9	32.1	30.4	28.9		
		1	33.7	31.8	30.1	28.5	27.1			
		1.25	29.9	28.3	26.8	25.4				
		1.5	26.6	25.2	24.0					
		1.75	23.8	22.6						
		2	21.4							
10		0.25	6.9	6.7	6.5	0.8	6.1	5.9	5.7	5.5
		0.5	6.5	6.2	6.0	0.7	5.7	5.5	5.3	
		0.75	6.0	5.8	5.6	0.7	5.3	5.1		
		1	5.6	5.4	5.3	0.6	5.0			
		1.25	5.3	5.1	4.9	0.6				
		1.5	4.9	4.8	4.6					
		1.75	4.6	4.5						
		2	4.3							
15		0.25	2.1	2.1	2.0	0.2	1.9	1.9	1.9	1.8
		0.5	2.0	2.0	1.9	0.2	1.9	1.8	1.8	
		0.75	1.9	1.9	1.8	0.2	1.8	1.7		
		1	1.8	1.8	1.8	0.2	1.7			
		1.25	1.8	1.7	1.7	0.2				
		1.5	1.7	1.6	1.6					
		1.75	1.6	1.6						
		2	1.5							

Table 6: The required practical resolution of the sensor for different configurations and targets in terms of the gravity difference in microGal which would need to be detected between the two sensors

Target Depth (m)	Sensor Height (m)	Target Radius (m)	0.5								1								2							
		Sensor Separation (m)	0.25	0.5	0.75	1	1.25	1.5	1.75	2	0.25	0.5	0.75	1	1.25	1.5	1.75	2	0.25	0.5	0.75	1	1.25	1.5	1.75	2
2	0.25		2.E-1	4.E-1	5.E-1	6.E-1	7.E-1	8.E-1	8.E-1	9.E-1	2.E+0	3.E+0	4.E+0	5.E+0	6.E+0	6.E+0	7.E+0	7.E+0	1.E+1	3.E+1	3.E+1	4.E+1	4.E+1	5.E+1	5.E+1	5.E+1
	0.5		2.E-1	3.E-1	4.E-1	5.E-1	5.E-1	6.E-1	6.E-1		1.E+0	2.E+0	3.E+0	4.E+0	4.E+0	5.E+0	5.E+0		1.E+1	2.E+1	3.E+1	3.E+1	3.E+1	4.E+1	4.E+1	
	0.75		1.E-1	2.E-1	3.E-1	4.E-1	4.E-1	5.E-1			1.E+0	2.E+0	2.E+0	3.E+0	3.E+0	4.E+0			8.E+0	1.E+1	2.E+1	2.E+1	3.E+1	3.E+1		
	1		1.E-1	2.E-1	2.E-1	3.E-1	3.E-1				8.E-1	1.E+0	2.E+0	2.E+0	3.E+0				6.E+0	1.E+1	2.E+1	2.E+1	2.E+1			
	1.25		8.E-2	1.E-1	2.E-1	2.E-1					6.E-1	1.E+0	2.E+0	2.E+0					5.E+0	9.E+0	1.E+1	2.E+1				
	1.5		6.E-2	1.E-1	2.E-1						5.E-1	9.E-1	1.E+0						4.E+0	7.E+0	1.E+1					
	1.75		5.E-2	1.E-1							4.E-1	8.E-1							3.E+0	6.E+0						
	2		4.E-2								3.E-1								3.E+0							
5	0.25		2.E-1	4.E-2	5.E-2	6.E-2	8.E-2	9.E-2	1.E-1	1.E-1	1.E+0	3.E-1	4.E-1	5.E-1	6.E-1	7.E-1	8.E-1	8.E-1	1.E+1	2.E+0	3.E+0	4.E+0	5.E+0	6.E+0	6.E+0	7.E+0
	0.5		2.E-2	3.E-2	5.E-2	6.E-2	7.E-2	8.E-2	8.E-2		1.E-1	3.E-1	4.E-1	5.E-1	5.E-1	6.E-1	7.E-1		1.E+0	2.E+0	3.E+0	4.E+0	4.E+0	5.E+0	5.E+0	
	0.75		1.E-2	3.E-2	4.E-2	5.E-2	6.E-2	7.E-2			1.E-1	2.E-1	3.E-1	4.E-1	5.E-1	5.E-1			1.E+0	2.E+0	3.E+0	3.E+0	4.E+0	4.E+0		
	1		1.E-2	2.E-2	4.E-2	4.E-2	5.E-2				1.E-1	2.E-1	3.E-1	4.E-1	4.E-1				8.E-1	2.E+0	2.E+0	3.E+0	3.E+0			
	1.25		1.E-2	2.E-2	3.E-2	4.E-2					9.E-2	2.E-1	3.E-1	3.E-1					7.E-1	1.E+0	2.E+0	3.E+0				
	1.5		1.E-2	2.E-2	3.E-2						8.E-2	2.E-1	2.E-1						7.E-1	1.E+0	2.E+0					
	1.75		9.E-3	2.E-2							7.E-2	1.E-1							6.E-1	1.E+0						
	2		8.E-3								7.E-2								5.E-1							
10	0.25		3.E-3	5.E-3	8.E-3	1.E-2	1.E-2	1.E-2	2.E-2	2.E-2	2.E-2	4.E-2	6.E-2	1.E-2	9.E-2	1.E-1	1.E-1	1.E-1	2.E-1	3.E-1	5.E-1	8.E-2	8.E-1	9.E-1	1.E+0	1.E+0
	0.5		3.E-3	5.E-3	7.E-3	9.E-3	1.E-2	1.E-2	1.E-2		2.E-2	4.E-2	6.E-2	9.E-3	9.E-2	1.E-1	1.E-1		2.E-1	3.E-1	5.E-1	7.E-2	7.E-1	8.E-1	9.E-1	
	0.75		2.E-3	5.E-3	7.E-3	9.E-3	1.E-2	1.E-2			2.E-2	4.E-2	5.E-2	9.E-3	8.E-2	1.E-1			2.E-1	3.E-1	4.E-1	7.E-2	7.E-1	8.E-1		
	1		2.E-3	4.E-3	6.E-3	8.E-3	1.E-2				2.E-2	3.E-2	5.E-2	8.E-3	8.E-2				1.E-1	3.E-1	4.E-1	6.E-2	6.E-1			
	1.25		2.E-3	4.E-3	6.E-3	7.E-3					2.E-2	3.E-2	5.E-2	7.E-3					1.E-1	3.E-1	4.E-1	6.E-2				
	1.5		2.E-3	4.E-3	5.E-3						2.E-2	3.E-2	4.E-2						1.E-1	2.E-1	3.E-1					
	1.75		2.E-3	4.E-3							1.E-2	3.E-2							1.E-1	2.E-1						
	2		2.E-3								1.E-2								1.E-1							
15	0.25		8.E-4	2.E-3	2.E-3	3.E-3	4.E-3	4.E-3	5.E-3	6.E-3	7.E-3	1.E-2	2.E-2	3.E-3	3.E-2	4.E-2	4.E-2	5.E-2	5.E-2	1.E-1	2.E-1	2.E-2	2.E-1	3.E-1	3.E-1	4.E-1
	0.5		8.E-4	2.E-3	2.E-3	3.E-3	4.E-3	4.E-3	5.E-3		6.E-3	1.E-2	2.E-2	3.E-3	3.E-2	3.E-2	4.E-2		5.E-2	1.E-1	1.E-1	2.E-2	2.E-1	3.E-1	3.E-1	
	0.75		8.E-4	1.E-3	2.E-3	3.E-3	3.E-3	4.E-3			6.E-3	1.E-2	2.E-2	3.E-3	3.E-2	3.E-2			5.E-2	9.E-2	1.E-1	2.E-2	2.E-1	3.E-1		
	1		7.E-4	1.E-3	2.E-3	3.E-3	3.E-3				6.E-3	1.E-2	2.E-2	3.E-3	3.E-2				5.E-2	9.E-2	1.E-1	2.E-2	2.E-1			
	1.25		7.E-4	1.E-3	2.E-3	3.E-3					6.E-3	1.E-2	2.E-2	3.E-3					4.E-2	9.E-2	1.E-1	2.E-2				
	1.5		7.E-4	1.E-3	2.E-3						5.E-3	1.E-2	2.E-2						4.E-2	8.E-2	1.E-1					
	1.75		6.E-4	1.E-3							5.E-3	1.E-2							4.E-2	8.E-2						
	2		6.E-4								5.E-3								4.E-2							

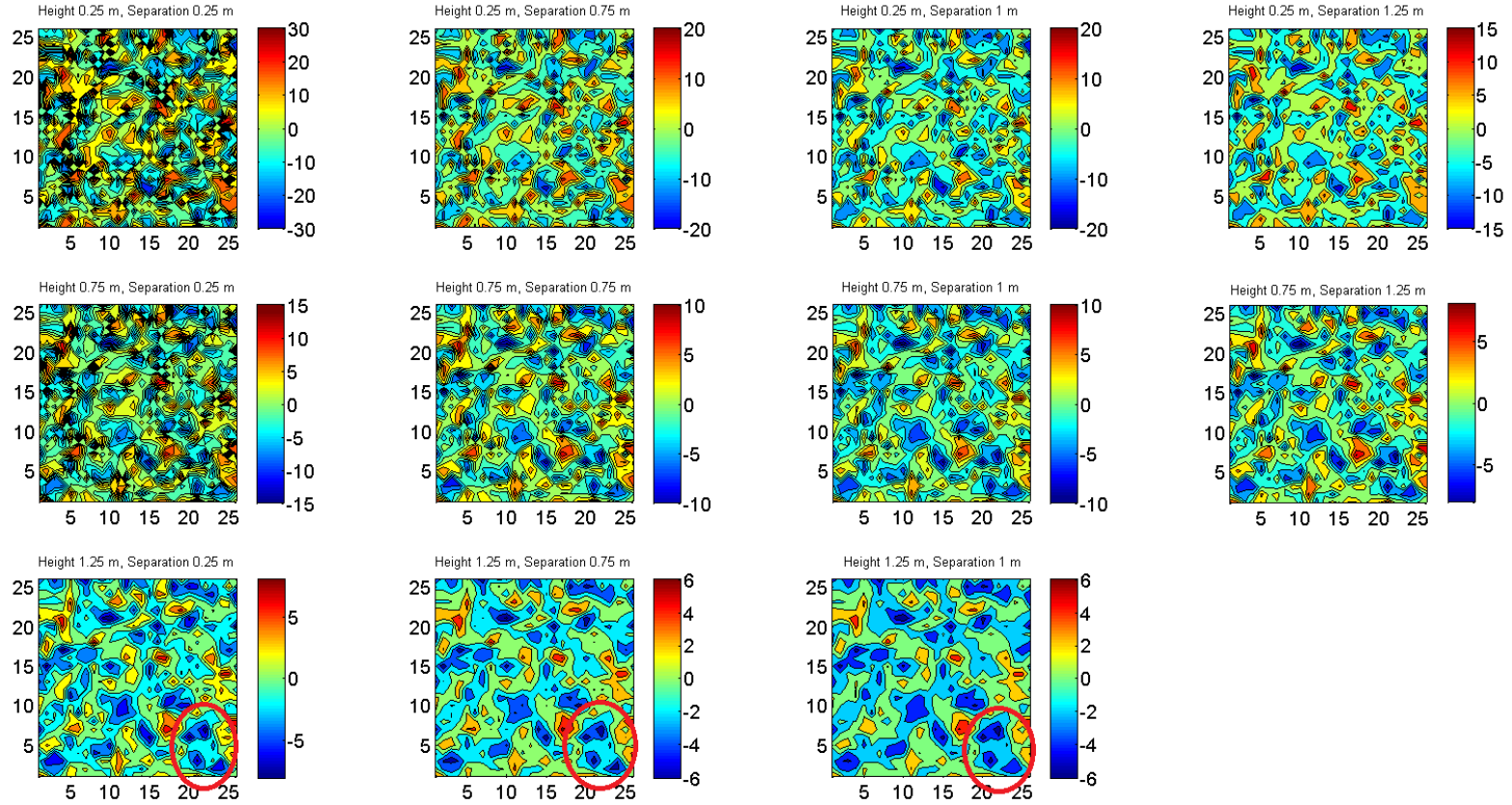

Figure 15: Gravity maps of soil noise for different gravity gradient instrument configurations in terms of sensor height and separation with contours every 2 Eötvos (note the differences in the scale bars between figures). Noise was generated using a side length of 0.8m and uniform random distribution over a 25 x 25 m grid with a measurement spacing of 1 m. A pattern of noise with a signal wavelength similar to a potential spherical void feature of interest indicated by the red oval is shown in the bottom right corner of the plots with the instrument at greater heights

However, whilst raising the instrument above the ground gives the greatest reduction in the overall noise amplitude, it greatly increases the requirements on instrument sensitivity (see Table 4) in order to detect features of interest, and averages the smaller scale variations into longer wavelength coherent signals. This can be easily mistaken for other features of interest due to their similar signal wavelengths as shown in Figure 15. Maintaining a clear distinction in the signal wavelength is important, not only because it makes the signals from the target of interest easier to see, but also allows spatial filtering methods to be used in order to suppress noise from near surface features. These bandpass filtering methods have been widely used in geophysics to suppress both near surface short wavelength noise (low pass filtering) and long wavelength geological noise (high pass filtering) (e.g. Clement, 1973; Zahra and Oweis, 2016) in the signal. However, further research is needed to determine optimum measurement and filtering strategies for high accuracy gravity surveys for a range of different targets. For these reasons, it is preferable and technologically more viable to tackle the instrument noise by increasing the measurement spacing between the top and bottom sensor. This has the advantage of relaxing the sensitivity requirement of the instrument (as the difference in gravity between the two sensors will be much larger) making the development of a suitable gravity gradient instrument easier, especially with current technological limitations on the precision and accuracy of QT gravity sensing technology (see for example those discussed by D'Amico et al., 2016; Freier et al., 2016) , such as for example the laser frequency and intensity stability.

5. Summary and Conclusions

Soil density variation and the resulting gravity signals, whilst currently obscured during microgravity surveys by other sources of noise and the limited practical resolution of the instruments, present an interesting and previously unquantified source of noise for measurements of subsurface targets with more accurate gravity and gravity gradient instruments. The variation of soil density both spatially as well as with depth were assessed from borehole records. Forward modelling was used to assess the impact of soil variation on gravity and gravity gradiometer measurements. The key findings were:

- Analysis of borehole data from two study areas in the UK showed that near surface variations are difficult to predict, both in terms of their spatial distribution and scale. Nevertheless, density variations with a range of 600-900 kg/m^3 were observed. The analysis showed that the densities were distributed between uniform and normal distributions with no clear dependency on the underlying soil type.
- Results of the forward simulations showed that soil noise will affect the new instruments significantly if predicted levels of practical resolution can be reached. Random density distribution models create noise at a significant level in the worst case scenarios for total field instruments (up to 5 μGal), and an even greater level for gravity gradiometers (up to 60 Eötvos) which may obscure the signal from the feature of interest.
- Soil noise can be suppressed through instrumental configuration and survey practice. Whilst increasing the height of the instrument was nearly twice as

effective at reducing the magnitude of soil noise compared with increasing the separation of the two atom clouds, increasing the separation may be the preferred solution as this both relaxes the sensitivity requirements of the sensor heads and avoids spreading the signal wavelengths of the noise into the similar signal wavelengths as potential buried targets, allowing them to be mistaken for additional features of interest or to mask existing ones.

- Keeping the noise within different spatial signal wavelengths also allows the possibility of spatial filtering, such as that widely used in other geophysical techniques to suppress geological or near surface features to be used in order to accentuate the signals from the target features and increase the likelihood of a successful survey.

6. Acknowledgements

The authors acknowledge the financial support provided by Innovate UK and the Engineering and Physical Sciences Research Council (EPSRC) through the “Study of Industrial Gravity Measurements and Applications + (SIGMA+) project” EP/M508378/1 and REVEAL project EP/R000220/1.

7. References

Boddice, D., Atkins, P., Rodgers, A., Metje, N., Goncharenko, Y. and Chapman, D. 2018. A novel approach to reduce environmental noise in microgravity measurements using a Scintrex CG5. Journal of Applied Geophysics 152, 221-235

Boddice, D., Metje, N. and Tuckwell, G. 2016. The Potential for Quantum Technology Gravity Sensors. In: The Potential for Quantum Technology Gravity Sensors, Vol. 18.

Boddice, D., Metje, N. and Tuckwell, G. 2017. Capability Assessment and Challenges for Quantum Technology Gravity Sensors for Near Surface Terrestrial Geophysical Surveying. Journal of Applied Geophysics 146, 149–159

British Geological Survey 2013. Digital Geological Map of Great Britain 1:10000 scale (DiGMapGB-10) data [SHAPE geospatial data] Tiles: ns56ne, ns56se, ns66nw, ns66sw (Glasgow) tq37ne, tq37nw, tq37se, tq37sw, tq38ne, tq38nw, tq38se, tq38sw, tq47ne, tq47nw, tq47se, tq47sw, tq48ne, tq48nw, tq48se, tq48sw, tq57ne, tq57nw, tq57se, tq57sw, tq58ne, tq58nw, tq58se, tq58sw, tq67ne, tq67nw ,tq67se, tq67sw, tq68ne, tq68nw, tq68se, tq68sw (London). British Geological Survey, UK. Downloaded: 2017-01-26 using EDINA Geology Digimap Service <http://digimap.edina.ac.uk>

Brown, G., Ridley, K., Rodgers, A. and de Villiers, G. 2016. Bayesian signal processing techniques for the detection of highly localised gravity anomalies using quantum interferometry technology. Proc. SPIE 9992 Emerging Imaging and Sensing Technologies, 99920M

BSI 1990. Methods of Test for Soils for Civil Engineering Purposes: Part 2: Classification Tests. In: Methods of Test for Soils for Civil Engineering Purposes: Part 2: Classification Tests. British Standards Institution.

Clement, W.G. 1973. Basic principles of two-dimensional digital filtering. Geophysical Prospecting 21, 125-145

D'Amico, G., Borselli, F., Cacciapuoti, L., Prevedelli, M., Rosi, G., Sorrentino, F. and Tino, G.M. 2016. Bragg interferometer for gravity gradient measurements. Physical Review A 93, 063628

Freier, C., Hauth, M., Schkolnik, V., Leykauf, B., Schilling, M., Wziontek, H., Scherneck, H.G., Müller, J. and Peters, A. 2016. Mobile quantum gravity sensor with unprecedented stability. Journal of Physics: Conference Series 723, 012050

Hendrickx, J., Borchers, B., Woolslayer, J., Dekker, L., Ritsema, C., Paton VI , S., Dubey, A., Harvey, J., Broach, J. and George, V. 2001. Spatial variability of dielectric properties in field soils. Detection and Remediation Technologies for Mines and Minelike Targets Orlando FL, 398-408

Hinton, A., Perea-Ortiz, M., Winch, J., Briggs, J., Freer, S., Moustoukas, D., Powell-Gill, S., Squire, C., Lamb, A., Rammeloo, C., Stray, B., Voulazeris, G., Zhu, L., Kaushik, A., Lien, Y.-H., Niggebaum, A., Rodgers, A., Stabrawa, A., Boddice, D., Plant, S.R., Tuckwell, G.W., Bongs, K., Metje, N. and Holynski, M. 2017. A portable magneto-optical trap with prospects for atom interferometry in civil engineering. Philosophical Transactions of the Royal Society A: Mathematical, Physical and Engineering Sciences 375,

Jiang, Z., Pálinkáš, V., Francis, O., Jousset, P., Mäkinen, J., Merlet, S., Becker, M., Coulomb, A., Kessler-Schulz, K.U., Schulz, H.R., Ch, R., Tisserand, L. and Lequin, D. 2012. Relative Gravity Measurement Campaign during the 8th International Comparison of Absolute Gravimeters (2009). Metrologia 49, 95

Muquans. 2017. *Muquans Absolute Quantum Gravimeter Product Page*. [cited 22/03/17]; Available from: https://www.muquans.com/index.php/products/aqg.

Niebauer, T.M., Sasagawa, G.S., Faller, J.E., Hilt, R. and Klopping, F. 1995. A new generation of absolute gravimeters. Metrologia 32, 159

Sherwood, P.T. 1970. *The reproducibility of the results of soil classification and compaction tests*. Road Research Laboratory, Earthworks and Foundations Section; [Reproduced by the Clearinghouse for Federal Scientific & Technical Information, Springfield, Va.], Crowthorne, Berk.

Telford, W.M., Geldart, L.P. and Sheriff, R.E. 1990. *Applied Geophysics*. Cambridge University Press.

Tuckwell, G., Grossey, T., Owen, S. and Stearns, P. 2008. The use of microgravity to detect small distributed voids and low-density ground. Quarterly Journal of Engineering Geology and Hydrogeology 41, 371-380

Van Dam, R., Hendrickx, J., Harrison, B., Borchers, B., Norman, D., Ndur, S., Jasper, C., Niemeyer, P., Nartey, R., Vega, D., Calvo, L., Simms, J.I., Harmon, R., Broach, J. and Holloway Jr, J. 2004. Spatial variability of magnetic soil properties. In: *Proc. Detection and Remediation Technologies for Mines and Minelike Targets, Orlando FL* (eds. R.S. Harmon, J.T. Broach and J.H. Holloway), pp. 665-676. Society of Photo-optical Instrumentation Engineers (SPIE).

Zahra, H.S. and Oweis, H.T. 2016. Application of high-pass filtering techniques on gravity and magnetic data of the eastern Qattara Depression area, Western Desert, Egypt. NRIAG Journal of Astronomy and Geophysics 5, 106-123

Appendix – BGS Rock Classification Scheme Abbreviation

The BGS rock classification scheme is a comprehensive system for classifying and naming geological materials to act as a corporate standard in support of their digital geological maps, data dictionaries, and numerous other modern geological applications. Further details on the BGS rock classification scheme can be found at http://www.bgs.ac.uk/bgsrcs/. The abbreviations used in the current work are defined below. Bedrock types are shown underlined**,** *Superficial geology types are shown in italics* and **Artificial or man-made deposits are shown in bold.**

Abbreviation	**Description**
ALV-C	Alluvium – Clay
ALV-Z	Alluvium – Clay and Silt
CAL-LMST	Calmy Limestone
GFDUD-XSV	Glaciofluvial Deposits, Devensian – Sand and Gravel
GOSA-XSV	Gourock Sand Member – Sand and Gravel
HEAD-C	Head – Clay
HEAD-XSC	Head – Sand and Clay
HWH-SANDU	Harwich Formation – Sand
KARN-XSV	*Killearn Sand and Gravel member – Sand and Gravel*
LC-Clay	London Clay Formation - Clay
LCMS-CYCCM	Scottish Lower Coal Measures Formation (Coal Measure Type)
LDE-C	Lacustrine Deposits - Clay
LHGR-XSV	Lynch Hill Gravel Member – Sand and Gravel
LMBE-CLAY	Lambeth Group – Clay
LMBE-SACL	Lambeth Group – Sandy Clay
LMBE-SANCL	Lambeth Group – Sand and Clay
LSC-CYCC	Limestone Coal Formation (Clackmannan Group Type)
MCMS-CYCCM	Scottish Middle Coal Measures Formation (Coal Measure Type)

MGR-ARTDP	Made Ground (Undivided) – Artificial Deposit
PAIS-XZC	Paisley Clay Member – Silt and Clay
RMDV-XCZ	Raised Marine Deposits, Devensian – Clay and Silt
RMDV- XSV	Raised Marine Deposits, Devensian – Sand and Gravel
SECK-CHLK	Seaford Chalk Formation – Chalk
SNCK-CHLK	Seaford Chalk Formation and Newhaven Chalk Formation (Undifferentiated) – Chalk
TAB-SANDU	Thanet Sand Formation – Sand
TILLD-DMTN	Till, Devensian - Diamicton
TPGR-V	Taplow Gravel Formation – Gravel
TPGR-XSV	Taplow Gravel Formation – Sand and Gravel
ULGS-CYCC	Upper Limestone Formation (Clackmannan Group Type)
WGR-UKNOWN	Worked Ground (Undivided) – Unknown or Unclassified Entry
WMGR-ARTDP	Infilled Ground – Artificial Deposit
WMGR- UKNOWN	Infilled Ground – Unknown or Unclassified Entry